Lowry OH, Rosebrough NJ, Farr AL, and Randall RJ (1951) Protein measurement with the Folin phenol reagent. *J Biol Chem* **193**:265–267

Matsushima S, Maeda K, Kondo C, Hirano M, Sasaki M, Suzuki H, and Sugiyama Y (2005) Identification of the hepatic efflux transporters of organic anions using double transfected MDCKII cells expressing human OATP1B1/MRP2, OATP1B1/MDR1 and OATP1B1/BCRP. *J Pharmacol Exp Ther* **314**:1059–1067.

Morikawa A, Goto Y, Suzuki H, Hirohashi T, and Sugiyama Y (2000) Biliary excretion of 17beta-estradiol 17beta-D-glucuronide is predominantly mediated by cMOAT/MRP2. *Pharm Res (NY)* **17**:546–552.

Nakai D, Nakagomi R, Furuta Y, Tokui T, Abe T, Ikeda T, and Nishimura K (2001) Human liver-specific organic anion transporter, LST-1, mediates uptake of pravastatin by human hepatocytes. *J Pharmacol Exp Ther* **297**:861–867.

Nishizato Y, Ieiri I, Suzuki H, Kimura M, Kawabata K, Hirota T, Takane H, Irie S, Kusuhara H, Urasaki Y, et al. (2003) Polymorphisms of OATP-C (SLC21A6) and OAT3 (SLC22A8) genes: consequences for pravastatin pharmacokinetics. *Clin Pharmacol Ther* **73**:554–565.

Shimizu M, Fuse K, Okudaira K, Nishigaki R, Maeda K, Kusuhara H, and Sugiyama Y (2005) Contribution of OATP (organic anion-transporting polypeptide) family transporters to the hepatic uptake of fexofenadine in humans. *Drug Metab Dispos* **33**:1477–1481.

Shitara Y, Itoh T, Sato H, Li AP, and Sugiyama Y (2003a) Inhibition of transporter-mediated hepatic uptake as a mechanism for drug-drug interaction between cerivastatin and cyclosporin A. *J Pharmacol Exp Ther* **304**:610–616.

Shitara Y, Li AP, Kato Y, Lu C, Ito K, Itoh T, and Sugiyama Y (2003b) Function of uptake transporters for taurocholate and estradiol 17beta-D-glucuronide in cryopreserved human hepatocytes. *Drug Metab Pharmacokinet* **18**:33–41.

Tamai I, Nezu J, Uchino H, Sai Y, Oku A, Shimane M, and Tsuji A (2000) Molecular identification and characterization of novel members of the human organic anion transporter (OATP) family. *Biochem Biophys Res Commun* **273**:251–260.

Vavricka SR, Van Montfoort J, Ha HR, Meier PJ, and Fattinger K (2002) Interactions of rifamycin SV and rifampicin with organic anion uptake systems of human liver. *Hepatology* **36**:164–172.

Waldmeier F, Flesch G, Muller P, Winkler T, Kriemler HP, Buhlmayer P, and De Gasparo M (1997) Pharmacokinetics, disposition and biotransformation of [14C]-radiolabelled valsartan in healthy male volunteers after a single oral dose. *Xenobiotica* **27**:59–71.

Yamaoka K, Tanigawara Y, Nakagawa T, and Uno T (1981) A pharmacokinetic analysis program (MULTI) for microcomputer. *J Pharmacobio-Dyn* **4**:879–885.

Yamazaki M, Akiyama S, Ni'inuma K, Nishigaki R, and Sugiyama Y (1997) Biliary excretion of pravastatin in rats: contribution of the excretion pathway mediated by canalicular multispecific organic anion transporter. *Drug Metab Dispos* **25**:1123–1129.

Address correspondence to: Dr. Yuichi Sugiyama, Department of Molecular Pharmacokinetics, Graduate School of Pharmaceutical Sciences, The University of Tokyo, 7-3-1 Hongo, Bunkyo-ku, Tokyo, 113-0033 Japan. E-mail: sugiyama@mol.f.u-tokyo.ac.jp

0026-895X/06/7003-887–896
MOLECULAR PHARMACOLOGY
U.S. Government work not protected by U.S. copyright
Mol Pharmacol 70:887–896, 2006

Vol. 70, No. 3
25494/3137121
Printed in U.S.A.

Regulation of the Expression of Human Organic Anion Transporter 3 by Hepatocyte Nuclear Factor 1α/β and DNA Methylation[S]

Ryota Kikuchi, Hiroyuki Kusuhara, Naka Hattori, Kunio Shiota, Insook Kim, Frank J. Gonzalez, and Yuichi Sugiyama

Department of Molecular Pharmacokinetics, Graduate School of Pharmaceutical Sciences (R.K., H.K., Y.S.), and Laboratory of Cellular Biochemistry, Department of Animal Resource Sciences/Veterinary Medical Sciences (N.H., K.S.), University of Tokyo, Tokyo, Japan; and Laboratory of Metabolism, National Cancer Institute, National Institutes of Health, Bethesda, Maryland (I.K., F.J.G.)

Received April 8, 2006; accepted June 20, 2006

ABSTRACT

Human organic anion transporter 3 (hOAT3/SLC22A8) is predominantly expressed in the proximal tubules of the kidney and plays a major role in the urinary excretion of a variety of organic anions. The promoter region of hOAT3 was characterized to elucidate the mechanism underlying the tissue-specific expression of hOAT3. The minimal promoter of hOAT3 was identified to be located approximately 300 base pairs upstream of the transcriptional start site, where there are canonical TATA and hepatocyte nuclear factor (HNF1) binding motifs, which are conserved in the rodent Oat3 genes. Transactivation assays revealed that HNF1α and HNF1β markedly increased hOAT3 promoter activity, where the transactivation potency of HNF1β was lower than that of HNF1α. Mutations in the HNF1 binding motif prevented the transactivation. Electrophoretic mobility shift assays demonstrated binding of the HNF1α/HNF1α homodimer or HNF1α/HNF1β heterodimer to the hOAT3 promoter. It was also demonstrated that the promoter activity of hOAT3 is repressed by DNA methylation. Moreover, the expression of hOAT3 was activated de novo by forced expression of HNF1α alone or both HNF1α and HNF1β together with the concomitant DNA demethylation in human embryonic kidney 293 cells that lack expression of endogenous HNF1α and HNF1β, whereas forced expression of HNF1β alone could not activate the expression of hOAT3. This suggests a synergistic action of the HNF1α/HNF1α homodimer or HNF1α/HNF1β heterodimer and DNA demethylation for the constitutive expression of hOAT3. These results indicate that the tissue-specific expression of hOAT3 might be regulated by the concerted effect of genetic (HNF1α and HNF1β) and epigenetic (DNA methylation) factors.

Tubular secretion plays a significant role in the urinary excretion of many compounds together with filtration in the glomeruli. Cumulative evidence suggests that organic anion transporter 1 (OAT1/SLC22A6) and organic anion transporter 3 (OAT3/SLC22A8) are predominantly involved in the tubular secretion of anionic drugs and drug metabolites as well as endobiotics at the basolateral membrane of the kidney proximal tubules (Van Aubel et al., 2000; Hasegawa et al., 2002, 2003; Robertson and Rankin, 2005; Sekine et al., 2006). Generation of Oat1 and Oat3 null mice confirmed an essential role for these transporters in the renal transport (Sweet et al., 2002; Eraly et al., 2006). In contrast to the functional characterization of these transporters, the regulatory mechanism of the basal expression of OAT1 and OAT3 remains to be elucidated.

In the present study, we focused on hepatocyte nuclear factor 1 (HNF1), consisting of two isoforms, HNF1α and HNF1β, as a key regulator of OAT3 expression. HNF1 is a homeodomain-containing factor that is expressed in the epithelia of a variety of organs, including liver, kidney, intestine, stomach, and pancreas (Blumenfeld et al., 1991; Mendel and Crabtree, 1991; Tronche and Yaniv, 1992). In the kidney, expression of HNF1α is confined to the proximal tubules,

This work was supported by a Health and Labor Sciences research grant from the Ministry of Health, Labor and Welfare for the Research on Advanced Medical Technology.

Article, publication date, and citation information can be found at http://molpharm.aspetjournals.org.

doi:10.1124/mol.106.025494.

[S] The online version of this article (available at http://molpharm.aspetjournals.org) contains supplemental material.

ABBREVIATIONS: OAT, organic anion transporter; HNF1, hepatocyte nuclear factor 1; h, human; PCR, polymerase chain reaction; m, mouse; EMSA, electrophoretic mobility shift assay; HEK, human embryonic kidney; DTT, dithiothreitol; 5azadC, 5-aza-2′-deoxycytidine; wt, wild-type HNF1 sequence; per, perfect consensus sequence; mut, mutated consensus sequence; RT, reverse transcription; GAPDH, glyceraldehyde-3-phosphate dehydrogenase; TBS-T, Tris-buffered saline/0.05% Tween 20; nt, nucleotide(s).

whereas that of HNF1β is observed along the tubular epithelial cells throughout the entire nephron (Lazzaro et al., 1992; Pontoglio et al., 1996). HNF1 is functionally composed of three domains: an N-terminal dimerization domain, a homeobox-like DNA-binding domain, and a C-terminal transactivation domain. Both the dimerization domain and the DNA-binding domain of HNF1α and HNF1β show high homologies, enabling them to form heterodimers as well as homodimers and to recognize the same DNA sequences (Mendel et al., 1991). In contrast, their transactivation domains are more divergent, and HNF1α is a more potent transactivator than HNF1β (Rey-Campos et al., 1991).

HNF1α is involved in the regulation of a number of hepatic genes, including albumin, α1-antitrypsin, and α- and β-fibrinogen (Mendel and Crabtree, 1991; Tronche and Yaniv, 1992), and also some of the transporters expressed predominantly in liver (Jung et al., 2001; Shih et al., 2001). The importance of HNF1α in kidney proximal tubules has become apparent after studies using two lines of HNF1α-null mice as well as conventional in vitro studies (Pontoglio et al., 1996; Lee et al., 1998). One line of HNF1α-null mice suffers from renal Fanconi syndrome, a defect in renal proximal tubule reabsorption, leading to glucosuria, aminoaciduria, phosphaturia, and polyuria. Indeed, HNF1α plays an essential role in the expression of sodium glucose cotransporter 2 and sodium/phosphate cotransporter 1, which are involved in the reabsorption of filtered glucose and phosphate from the urine, respectively (Pontoglio et al., 2000; Cheret et al., 2002).

In contrast to HNF1α, the role of HNF1β in adult animals remains unclear, because the homologous inactivation of the HNF1β gene results in embryonic lethality at embryonic day 7.5 as a result of a defect in visceral endoderm differentiation (Barbacci et al., 1999; Coffinier et al., 1999). However, more recently, HNF1β was shown to be essential for the formation of a functional bile duct system and several hepatic metabolic functions, by means of the conditional gene-targeting technique (Coffinier et al., 2002). HNF1β is also involved in the regulation of kidney-specific Ksp-cadherin promoter (Bai et al., 2002), and kidney-specific inactivation of HNF1β leads to a renal polycystic phenotype (Gresh et al., 2004).

Because multiple CpG dinucleotides, primary targets of DNA methylation in the vertebrate genome, are located in the putative promoter region of hOAT3 (Fig. 1), we also focused on the role of DNA methylation in regulation of hOAT3 expression. DNA methylation is one of the mechanisms underlying the epigenetic control of gene expression (Bird, 2002). Methylation of the CpG dinucleotides in the promoter region can evoke the condensed structure of chromatin in the neighboring region through the recruitment of chromatin remodeling factors, such as methyl CpG binding proteins and histone deacetylases, which prevents transactivation by most of the transcription factors. Therefore, there is an inverse correlation between gene expression and DNA methylation in the promoter region. During the last decade, the role of DNA methylation in mammalian embryogenesis, differentiation, and progression of cancer has been highlighted. More recently, DNA methylation has been recognized to regulate the tissue-specific expression of many genes (Shiota, 2004). Whether these epigenetic mechanisms are involved in the regulation of transporter genes has remained largely unknown.

In the present study, we report the isolation of the hOAT3 promoter and demonstrate the involvement of HNF1α and HNF1β in basal transcriptional activity. In addition, these studies revealed that DNA methylation is involved in the gene suppression of hOAT3, and transcriptional activation of hOAT3 by HNF1α and HNF1β requires concomitant DNA demethylation of the promoter.

Materials and Methods

Materials. All reagents were purchased from Wako Pure Chemicals (Osaka, Japan) unless stated otherwise.

Isolation of the 5′-Flanking Region of the hOAT3 and mOat3 Gene. The transcriptional start site of the hOAT3 gene was identified using the public database Database of Transcriptional Start Sites (http://dbtss.hgc.jp/), with the ref sequence identification for hOAT3 (GenBank accession number NM_004254). DNA fragments of varying length from the 5′-flanking region of the hOAT3 gene were generated by polymerase chain reaction (PCR) using human genomic DNA as a template and the following primer sets:

Fig. 1. Multiple alignment of the putative proximal promoter of human, mouse, and rat OAT3. Nucleotide sequences of the 5′-flanking region of human (top), mouse (middle), and rat (bottom) OAT3 genes were aligned using Genetyx-Mac version 10 (Genetyx, Tokyo, Japan), so that the maximal homology of sequences among species could be obtained. Nucleotide numberings are relative to the transcriptional start sites (nt +1, arrow). Homologous sequences among species are boxed. Representative consensus binding motifs for putative regulatory elements are shaded with the respective transcription factors given above the sequence, and CpG dinucleotides in each sequence are reverse-colored.

forward, −1471, −644, or −308, and reverse +6 (Table 1). The primers were designed according to the sequence of the 5′-flanking region of the hOAT3 gene, and the number indicates the position of the primers relative to the transcriptional start site. The forward primers contained an artificial KpnI site and the reverse primers contained an artificial HindIII site. The resulting PCR products (−1471/+6, −644/+6, and −308/+6) were digested with KpnI and HindIII after subcloning into pGEM-T Easy vector (Promega, Madison, WI) and ligated into pGL3-Basic vector (Promega) predigested with KpnI and HindIII, yielding the following promoter constructs: −1471/+6-Luc, −644/+6-Luc, and −308/+6-Luc. The −35/+6-Luc construct was generated by in vitro annealing of the sense (−35/+6) and antisense (+6/−35) oligonucleotides (Table 1) followed by ligation into the pGL3-Basic vector that had been predigested with KpnI and HindIII. The mOat3 promoter fragment was PCR-amplified from mouse genomic DNA using the following primers: forward (−156) and reverse (+6) (Table 1). The amplified product was ligated into the pGL3-Basic vector as in the case of hOAT3, yielding the mOat3-Luc promoter construct. The sequence identity of all the constructs with the respective genomic sequences was verified by DNA sequencing. Plasmid DNA was prepared using the GenElute Plasmid Midiprep kit (Sigma-Aldrich, St. Louis, MO).

Plasmid Constructions. To generate HNF1α and HNF1β expression vectors, the coding regions of human HNF1α and HNF1β were amplified by PCR using primers containing HindIII and EcoRI restriction sites and inserted into the same sites of pcDNA3.1(+) vector (Invitrogen, Carlsbad, CA). The sequences of primers used for the amplification of HNF1α and HNF1β are listed in Table 1. The entire sequences were verified by DNA sequencing.

Site-Directed Mutagenesis. The mutated promoter fragment (−308/+6-HNF1mut) having a 4-base pair disrupted HNF1 motif was generated using the QuikChange XL site-directed mutagenesis kit (Stratagene, La Jolla, CA) using internal mutated oligonucleotides (Table 1). The introduction of the mutations was verified by DNA sequencing.

In Vitro Methylation of Plasmid DNA. Reporter constructs of the hOAT3 promoter were methylated in vitro with 3 U of SssI methylase (New England Biolabs, Beverly, MA) for each microgram of DNA in the presence of 160 μM *S*-adenosylmethionine at 37°C for 3 h. Completion of the methylation was confirmed by resistance to HpaII digestion (data not shown).

Cell Culture and Transfections. HepG2 and Caco-2 cell lines were maintained in a culture medium consisting of Dulbecco's modified Eagle's medium with 4500 mg/l glucose (Invitrogen) supplemented with 10% fetal bovine serum (Sigma-Aldrich), nonessential amino acids, 100 U/ml penicillin, and 100 μg/ml streptomycin (Invitrogen). The HEK293 cell line was maintained in a culture medium consisting of Dulbecco's modified Eagle's medium with 1000 mg/l glucose supplemented with 10% fetal bovine serum, 100 U/ml penicillin, and 100 μg/ml streptomycin. Cells were seeded in 24-well culture plates (0.5×10^5 cells/well) 1 day before transfection. HepG2 and Caco-2 cells were transfected with 0.5 μg of the corresponding promoter construct and 0.05 μg of the internal standard pRL-SV40 vector (Promega) to normalize the transfection efficiency using Lipofectamine 2000 (Invitrogen) according to the manufacturer's instructions. HEK293 cells were transfected with 0.5 μg of the corresponding promoter and 0.05 μg of pRL-SV40 using FuGENE 6 (Roche Diagnostics, Indianapolis, IN). For cotransfection assays with HEK293 cells, 0 to 0.5 μg of HNF1α and HNF1β expression vectors or empty pcDNA3.1(+) vector was added to the transfection reaction. Then, 48 h after transfection, cells were lysed with passive lysis buffer, and the luciferase activities were assayed using the dual-luciferase reporter system (Promega) and quantified in a Lumat LB 9507 luminometer (Berthold, Bad Wildbad, Germany). The promoter activity was measured as the relative light units of firefly luciferase per unit of *Renilla reniformis* luciferase.

TABLE 1

Oligonucleotides used for the production of promoter fragments, plasmid construction, mobility shift assays, site-directed mutagenesis, RT-PCR, and quantitative PCR

Regarding the oligonucleotides used for the mobility shift assays and site-directed mutagenesis, the HNF1 recognition motif in the hOAT3 promoter region is underlined. Bold type indicates the difference in the sequence of the per and mut compared with wt sequence found in the hOAT3 promoter.

Oligonucleotide	Orientation	Sequence (5′ to 3′)
Primers and oligonucleotides used for cloning of 5′-flanking regions		
hOAT3		
−1471	Forward	CGGGGTACCGGAACAGAGAGGTAAAGGC
−644	Forward	CGGGGTACCGAGAGAAGCCTGTCCATTG
−308	Forward	CGGGGTACCGATTCCTTCCCAGAATCTCC
+6	Reverse	CCCAAGCTTCAAGCTGTGTTTGTGCCTCC
−35/+6	Sense	CCCTTATATAAGCCCCCCTGGGGGAGGCACAAACACAGCTTGA
+6/−35	Antisense	AGCTTCAAGCTGTGTTTGTGCCTCCCCCAGGGGGGCTTATATAAGGGGTAC
mOat3		
−156	Forward	CGGGGTACCATCAACAGCCTTGGCTGAGG
+6	Reverse	CCCAAGCTTCAAGCTGTTTGTGTCTCC
Primers used for cloning of HNF1α and HNF1β		
HNF1α	Forward	AAGCTTGCCATGGTTTCTAAACTGAGCC
	Reverse	GAATTCTGGTTACTGGGAGGAAGAGGCC
HNF1β	Forward	AAGCTTGAAAATGGTGTCCAAGCTCACG
	Reverse	GAATTCGGCATCACCAGGCTTGTAGAGG
Oligonucleotides used for construction of EMSA probe and competitor or site-directed mutagenesis		
wt	Sense	CGCAAAAGAAAGTCAAACATTAGCCCGGGAAACAGC
per	Sense	CGCAAAAGAAAGTTAATCATTAACCCGGGAAACAGC
mut	Sense	CGCAAAAGAAAGTCACACATCGCCCCGGGAAACAGC
Primers used for RT-PCR or quantitative PCR		
hOAT3	Forward	GGCAGGTATACTGATTGGAG
	Reverse	TCCACCAGGATGATAGGAAG
HNF1α	Forward	TGGGTCCTACGTTCACCAAC
	Reverse	TCTGCACAGGTGGCATGAGC
HNF1β	Forward	TGCACAAAGCCTCAACACCT
	Reverse	GTTGGTGAGTGTACTGATGC
GAPDH	Forward	AATGACCCCTTCATTGAC
	Reverse	TCCACGACGTACTCAGCGC

Preparation of Nuclear Extracts. Nuclear extracts were prepared from 1.0×10^7 of HepG2, Caco-2, and HEK293 cells. Cell centrifugation and the subsequent steps to recover the nuclear proteins were all performed at 4°C. Cells were scraped off the plates, suspended in 0.5 ml of phosphate-buffered saline, and centrifuged at 1500*g* for 5 min. The cellular pellet was resuspended in 150 μl of buffer A (10 mM HEPES, pH 7.9, 10 mM KCl, 0.2 mM EDTA, 0.4% Nonidet P-40, 1 mM DTT, 0.5 mM phenylmethylsulfonyl fluoride, and 1% protease inhibitor cocktail; Sigma-Aldrich). After a 10-min incubation on ice, cells were centrifuged at 4°C and 3000 rpm for 5 min. The pellet was resuspended in 150 μl of buffer A and centrifuged at 4°C and 3000 rpm for 5 min, and this process was repeated twice. The supernatant was removed, and the nuclear pellet was resuspended in 200 μl of buffer B (20 mM HEPES, pH 7.9, 400 mM NaCl, 2 mM EDTA, 1 mM DTT, 0.5 mM phenylmethylsulfonyl fluoride, and 1% protease inhibitor cocktail) and incubated on ice for 30 min. The tube was centrifuged at 4°C and 10,000 rpm for 20 min, and the supernatant was recovered as the nuclear extract. Protein concentrations were measured by the method of Lowry et al. (1951).

Electrophoretic Mobility Shift Assay. The double-stranded oligonucleotide probes were obtained by hybridizing single-stranded complementary oligonucleotides with sense sequences as shown in Table 1. Digoxigenin-11-ddUTP was incorporated into each 3′ end using a Dig Gel Shift kit, 2nd Generation (Roche Diagnostics). Sequence wt corresponds to the wild-type HNF1 sequence found in the hOAT3 promoter, and per corresponds to the perfect consensus sequence for HNF1, whereas mut denotes the wild-type sequence mutated within the HNF1 recognition motif. For EMSA, 5 μg of nuclear extracts from HepG2, Caco-2, and HEK293 cells was incubated at room temperature for 15 min with 30 fmol of digoxigenin-labeled probe, 2 μg of poly(dI-dC), and 0.1 μg of poly-L-lysine in 20 μl of 20 mM HEPES, pH 7.6, 1 mM EDTA, 10 mM $(NH_4)_2SO_4$, 1 mM DTT, 2% (w/v) Tween 20, and 30 mM KCl. For competition assays, a 25-fold excess of unlabeled dimerized oligonucleotides was added. For supershift experiments, 1 μg of antibody against HNF1α or HNF1β (Santa Cruz Biotechnology, Inc., Santa Cruz, CA) was added to the reaction mixture. Reactions were analyzed by electrophoresis through Novex 6% DNA retardation gels (Invitrogen). After electrotransfer to a positively charged nylon membrane (Roche Diagnostics), bands were detected nonisotopically with a Dig Gel Shift kit, 2nd Generation, according to the manufacturer's instructions.

5-Aza-2′-deoxycytidine Treatment and Analysis of hOAT3 Expression by Reverse Transcription-PCR. Before the treatment with 5-aza-2′-deoxycytidine (5azadC) (DNA methylation inhibitor; Sigma-Aldrich), HepG2, Caco-2, and HEK293 cells were precultured for 24 h and then cultured for 72 h in medium containing 0, 1, 10, or 100 μM 5azadC. To examine the synergetic effect of the expression of HNF1α or HNF1β and DNA demethylation, HEK293 cells were plated in 24-well plates (0.5×10^5 cells/well) 1 day before transient transfection of 0 to 0.5 μg of HNF1α expression vector, HNF1β expression vector, or empty pcDNA3.1(+) vector. The transfection was performed using FuGENE 6 according to the manufacturer's instructions. After 12 h, the cells were treated with 0 or 100 μM 5azadC, cultured for 48 h, and then subjected to RNA isolation. Total RNA was prepared from cells by a single-step guanidium thiocyanate procedure using ISOGEN (Nippon Gene, Toyama, Japan). The RNA was then reverse-transcribed using a random-nonamer primer (Takara, Shiga, Japan). PCR was performed with the forward and reverse primers listed in Table 1 to detect the partial fragments of hOAT3, HNF1α, HNF1β, and GAPDH cDNA. PCR was performed under the following conditions: 94°C for 2 min; 40 cycles for hOAT3, 30 cycles for HNF1α and HNF1β, and 25 cycles for GAPDH of 94°C for 30 s, 55°C for 30 s, and 72°C for 1 min; final extension 72°C for 5 min.

Quantitative PCR. To quantify the mRNA expression of HNF1α and HNF1β in HepG2, Caco-2, and HEK293 cells, real-time quantitative PCR was performed using a LightCycler and the appropriate software (version 3.53; Roche Diagnostics) according to the manufacturer's instructions. cDNA used for the quantification was prepared as described above. Primers for HNF1α and HNF1β used in this study are shown in Table 1.

PCR was performed using a SYBR Premix Ex *Taq* (perfect real time) (Takara). The protocol for PCR was as follows: 95°C for 30 s, 40 cycles of 95°C for 5 s, 55°C for 10 s, and 72°C for 15 s. A standard curve was generated by dilutions of the target PCR product, which had been purified and had its concentration measured. To confirm the amplification specificity, the PCR products were subjected to a melting curve analysis. The mRNA expression of HNF1α and HNF1β in each cell line was normalized by the mRNA expression of GAPDH.

Western Blotting. Nuclear extracts prepared from HepG2 or Caco-2 cells were subjected to Western blot analysis to confirm the expression of HNF1α and HNF1β at protein levels. In this, 30 μg of nuclear proteins was electrophoresed on 10% SDS-polyacrylamide gel with a 4.4% stacking gel. Separated proteins were transferred to a polyvinylidene difluoride membrane using a blotter at 15 V for 1 h. The membrane was blocked with Tris-buffered saline/0.05% Tween 20 (TBS-T) and 5% skimmed milk for 1 h at room temperature and subsequently incubated with an antibody against HNF1α or HNF1β (1:2000) at 4°C overnight. After washing three times with TBS-T for 5 min, the membrane was allowed to bind a horseradish peroxidase-labeled donkey anti-goat IgG (Chemicon International, Temecula, CA) diluted 1:5000 in TBS-T for 1 h at room temperature and detected using ECL Plus (GE Healthcare, Little Chalfont, Buckinghamshire, UK).

Results

Computational Analysis of the Potential Transcription Factor Binding Sites in hOAT3, mOat3, and rOat3 Minimal Promoters. Sequence homologies to known gene regulatory elements in the hOAT3 5′-flanking region up to approximately nt −300 relative to the transcription start site were identified by a computer-based approach using Mat Inspector (http://www.genomatix.de/) (Fig. 1). Several potential transcription factor recognition sites were found in this region, including a TATA motif at nt −32 to −27, an HNF1 binding motif at nt −65 to −53, a cAMP response element-binding protein binding motif at nt −87 to −80, and a signal transducer and activator of transcription 5 binding motif at nt −302 to −294. In addition, there are 13 CpG dinucleotides in this region, which may be potential DNA methylation sites (Fig. 1). A homologous sequence to the hOAT3 5′-flanking region in the mouse and rat Oat3 genomic locus was obtained from the National Center for Biotechnology Information genome database. The transcriptional start site of mOat3 and rOat3 gene was suggested based on the high homology (approximately 70%) to the hOAT3 5′-flanking region (Fig. 1). The TATA motif and HNF1 motif were also found in the mOat3 and rOat3 putative promoters.

Analysis of Basal hOAT3 Gene Promoter Activity. To determine the minimal region of the hOAT3 proximal promoter required for its promoter activity, a series of deleted promoter constructs (−1471/+6-Luc, −644/+6-Luc, −308/+6-Luc, and −35/+6-Luc) were transfected into three kinds of human-derived cell lines (HepG2, Caco-2, and HEK293), and the luciferase activity in each cell line was measured (Fig. 2). The transfection of −1471/+6, −644/+6, and −308/+6 constructs resulted in increased luciferase activity compared with the promoterless pGL3-Basic plasmid in all cell lines, whereas no significant luciferase activity was observed after transfection of the −35/+6 construct. These

results suggest that −308 to +6 of the hOAT3 5′-flanking region can act as a minimal promoter. The luciferase activity of the −644/+6 construct was much lower than that of the −308/+6 construct only in HepG2 cells, suggesting the existence of some negative regulatory elements between −644 and −308 in this liver-derived tumor cell line.

Expression Level of HNF1α and HNF1β in HepG2, Caco-2, and HEK293 Cells. Real-time quantitative PCR revealed that the expression level of HNF1β in HepG2 cells was 27% that of HNF1α (Fig. 3A). The levels of HNF1α and HNF1β mRNA in Caco-2 cells were 73 and 55% that of HNF1α in HepG2 cells, respectively. In contrast, neither HNF1α nor HNF1β was detected in HEK293 cells. Western blot analysis with nuclear extracts from HepG2 or Caco-2 cells demonstrated that in HepG2 cells, HNF1α is predominantly expressed at the protein level, whereas in Caco-2 cells, both HNF1α and HNF1β are expressed (Fig. 3B).

Mutagenesis of the HNF1 Binding Motif. To investigate the functional importance of the HNF1 binding motif in the hOAT3 promoter region for the basal promoter activity, mutations in this motif were introduced into the −308/+6-Luc construct, and the reporter activity was measured after transfection into HepG2, Caco-2, and HEK293 cells (Fig. 4). Mutations in the HNF1 binding motif attenuated the luciferase activity by approximately 50% compared with the wild-type construct in HepG2 and Caco-2 cells where endogenous HNF1α and HNF1β were detected by real-time quantitative PCR. In contrast, HNF1 motif disruption by site-directed mutagenesis had no effect on the transcriptional activity in HNF1α- and HNF1β-deficient HEK293 cells. These results confirm that the HNF1 binding motif in the hOAT3 promoter is functional.

Transactivation of the Promoter Activity by Exogenous Expression of HNF1α and/or HNF1β. The effect of exogenously expressed HNF1α and HNF1β on the hOAT3 promoter activity was investigated by cotransfection assays in HEK293 cells. As shown in Fig. 5, independent or simultaneous transfection of HNF1α and HNF1β enhanced the luciferase activity of the hOAT3 −308/+6 wild-type reporter construct (−308/+6-HNF1wt) compared with the pcDNA3.1(+)-transfected control. The luciferase activities of the promoterless pGL3-Basic or hOAT3 −308/+6 HNF1-mutated reporter construct (−308/+6-HNF1mut) were not stimulated by transfection of the HNF1α and/or HNF1β expression vectors. These results provide clear evidence that both HNF1α and HNF1β can transactivate the basal promoter activity of hOAT3 and that the effect is mediated by the intact HNF1 binding motif in the hOAT3 promoter. The luciferase activity of the wild-type reporter construct with the independent transfection of HNF1α is higher than that

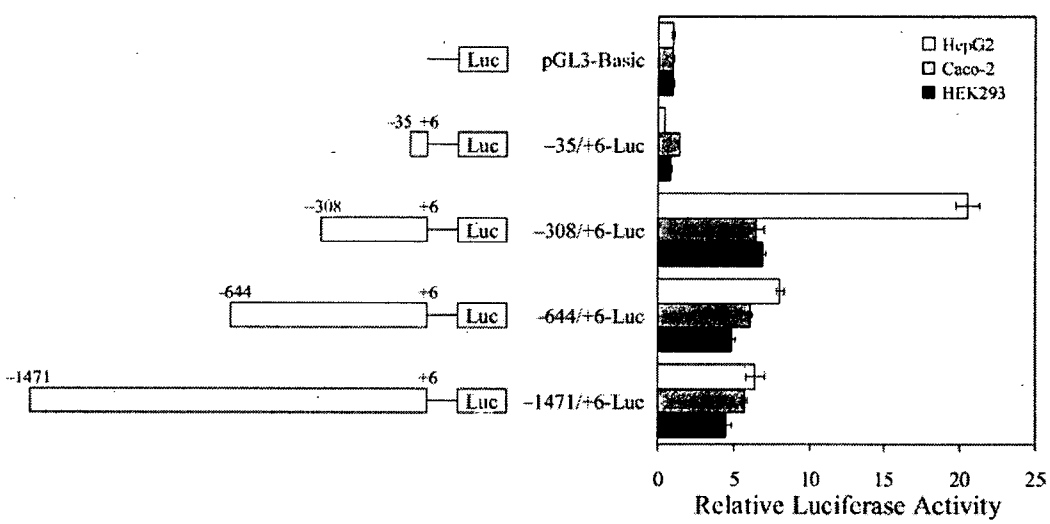

Fig. 2. Analysis of hOAT3 promoter function. HepG2 (white bars), Caco-2 (gray bars), and HEK293 cells (black bars) were transiently transfected with a series of deleted promoter constructs −35/+6-Luc, −308/+6-Luc, −644/+6-Luc, and −1471/+6-Luc, or a promoterless pGL3-Basic plasmid as described under *Materials and Methods*. Transfection efficiency was normalized by cotransfection of internal standard pRL-SV40. The promoter activity was measured as described under *Materials and Methods* and was shown as the factor of induction of luciferase over background activity measured in cells transfected with pGL3-Basic in each cell line. Results are presented as the mean ± S.E. of triplicate samples.

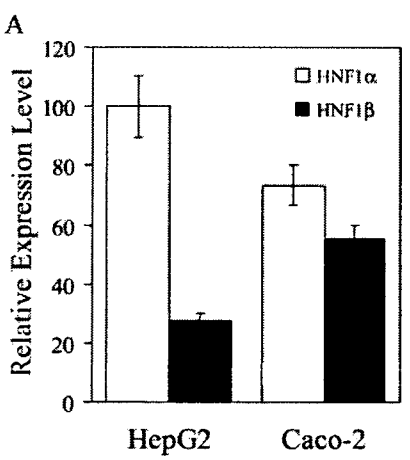

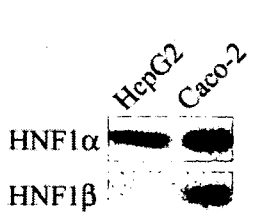

Fig. 3. Expression of HNF1α and HNF1β in HepG2, Caco-2, and HEK293 cells. A, mRNA expression of HNF1α and HNF1β was measured by real-time quantitative PCR using specific primers (Table 1), and the data were normalized by the mRNA expression of GAPDH. The relative expression level of HNF1α (white columns) and HNF1β (black columns) in each cell line was given as a ratio with respect to the mRNA expression of HNF1α in HepG2 cells which was taken as 100%. Results are presented as the mean ± S.E. of three samples. B, Western blotting was performed to investigate the protein expression of HNF1α and HNF1β. Nuclear extracts from HepG2 or Caco-2 cells were separated by SDS-polyacrylamide gel electrophoresis (10% separating gel), and HNF1α and HNF1β were detected as described under *Materials and Methods*.

with the independent transfection of HNF1β, indicating that the transactivation potency of HNF1β is lower than that of HNF1α. Simultaneous transfection of HNF1α and HNF1β yielded intermediate luciferase activity, which may be explained by the formation of a HNF1α/HNF1β heterodimer that enhances the promoter activity to the lesser degree than the HNF1α/HNF1α homodimer.

HNF1 Binds to the hOAT3 Promoter. EMSA was performed using the oligonucleotide probe corresponding to the −76/−41 region of the hOAT3 promoter, which includes the HNF1 binding motif and the nuclear extracts from HepG2, Caco-2, and HEK293 cells to show direct binding of HNF1α or HNF1β to the promoter (Fig. 6A). Incubation of the −76/−41 oligonucleotide probe with nuclear extracts from three cell lines resulted in three shifted bands (*a*, *b*, and *c*). The band *a* was observed when the probe was incubated with the nuclear extract from HepG2 cells (lane 2), and an additional band (band *b*) showing faster mobility was detected when the probe was incubated with the nuclear extracts from Caco-2 cells (lane 5). Band *c* was produced by incubation with the nuclear extract from each cell line (lanes 2, 5, and 8). The formation of bands *a* and *b* was abolished by an excess of unlabeled HNF1 consensus oligonucleotide (per) (lanes 3 and 6), but it was unaffected by the mutated oligonucleotide (mut) (lanes 4 and 7). These results suggest that the bands *a* and *b* can be ascribed to the binding of HNF1α or HNF1β to the −76/−41 oligonucleotide probe.

To confirm the specificity of HNF1 binding, supershift analysis was performed with HepG2 and Caco-2 nuclear extracts using a specific antibody to HNF1α or HNF1β (Fig. 6B). Band *a* was supershifted by the addition of an antibody to HNF1α but not by an antibody to HNF1β (lanes 3, 4, 6, and 7), whereas band *b* observed only in Caco-2 cells was supershifted by the addition of either of the antibodies (lanes 6 and 7). Thus, band *a* corresponds to HNF1α/HNF1α homodimer, and band *b* corresponds to HNF1α/HNF1β heterodimer. A previous report has shown that HNF1β/HNF1β homodimer migrating faster than HNF1α/HNF1β heterodimer may exist when both isoforms are present (Rey-Campos et al., 1991). However, in the present study, the formation of HNF1β/HNF1β homodimer was not clearly observed in Caco-2 cells where both isoforms were detected. The band *c* is ascribed to some nonspecific binding to the labeled probe, because this band was not abolished by the addition of unlabeled oligonucleotides. Taken together, these data suggest that the protein complex binding to the hOAT3 HNF1 motif in HepG2 cells is HNF1α/HNF1α homodimer and those in Caco-2 cells include HNF1α/HNF1β heterodimer as well as HNF1α/HNF1α homodimer. The difference in the band pattern is probably due to the different protein expression pattern of HNF1α and HNF1β in the two cell lines (Fig. 3B).

Transcriptional Activation of mOat3 Promoter by HNF1α and HNF1β. To investigate whether HNF1α or HNF1β is also involved in the promoter activity of mOat3, the proximal putative promoter of mOat3 was cloned into pGL3-Basic vector using the PCR-based approach, and the promoter activity of this reporter construct was measured in HepG2, Caco-2, and HEK293 cells. The luciferase activity of the mOat3 −156/+6 promoter construct (mOat3-Luc) was 6.5- and 3.6-fold higher than the promoterless pGL3-Basic plasmid in HepG2 and Caco-2 cells, respectively, whereas the activity in HEK293 cells was not significant (Supplemental Data A). Exogenous expression of HNF1α or HNF1β in HEK293 cells enhanced the promoter activity of mOat3 (Supplemental Data B). These observations suggest that the functional importance of HNF1α and HNF1β for the basal transcription of OAT3 genes is conserved among species.

Repression of hOAT3 Promoter Activity by DNA Methylation. To investigate the possible role of DNA methylation on the transcriptional repression of hOAT3, hOAT3 −308/+6 promoter construct was methylated in vitro; transfected into HepG2, Caco-2, and HEK293 cells; and the luciferase activity was measured. The transcriptional activity of hOAT3 was dramatically reduced by in vitro methylation of the promoter construct (Fig. 7). These data indicate that the

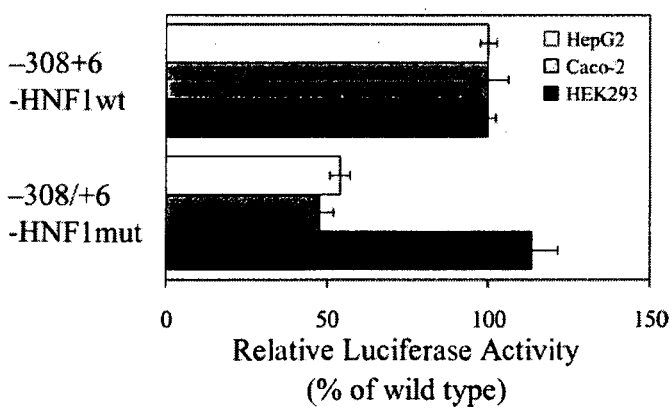

Fig. 4. Effect of mutations in the HNF1 binding motif on the hOAT3 promoter activity. HepG2 (white bars), Caco-2 (gray bars), and HEK293 cells (black bars) were transfected with wild-type (−308/+6-HNF1wt) or mutated (−308/+6-HNF1mut) promoter construct, and the luciferase activity was measured as described under *Materials and Methods*. The relative luciferase activity of the mutated construct is shown as a percentage of the wild-type construct in each cell line. Results are presented as the mean ± S.E. of triplicate samples.

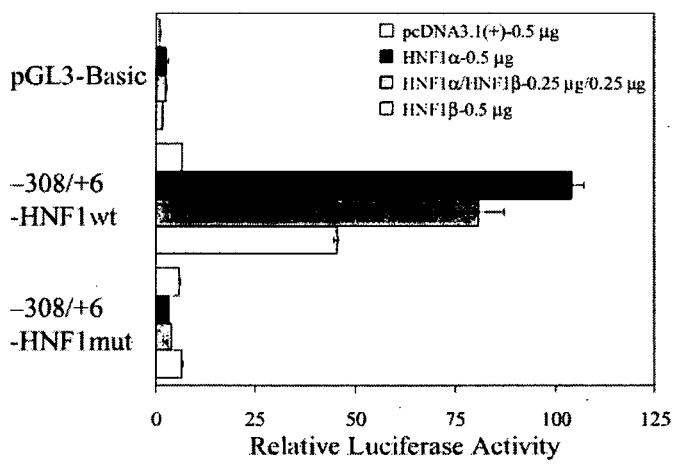

Fig. 5. Effect of exogenously expressed HNF1α and HNF1β on hOAT3 promoter function in HEK293 cells. HEK293 cells were transfected with wild type (−308/+6-HNF1wt) or mutated (−308/+6-HNF1mut) promoter construct, or a promoterless pGL3-Basic plasmid, together with 0.5 μg/well empty pcDNA3.1(+) vector (white bars), 0.5 μg/well HNF1α expression vector (black bars), 0.25 μg/well HNF1α and HNF1β expression vectors (gray bars), or 0.5 μg/well HNF1β expression vector (light gray bars). The luciferase activity was measured as described under *Materials and Methods* and was shown as the factor of induction over background activity measured in cells transfected with pGL3-Basic together with pcDNA3.1(+). Results are presented as the mean ± S.E. of triplicate samples.

expression of hOAT3 can be suppressed at a transcriptional level by DNA methylation.

Activation of hOAT3 Transcription by 5azadC Treatment in Nonexpressing Cell Lines. Expression of the endogenous hOAT3 gene in HepG2, Caco-2, and HEK293 cells is below the detection limit. To investigate whether the hOAT3 gene could be activated by DNA demethylation in these nonexpressing cell lines, the total RNA from each cell line treated with 5azadC, an inhibitor for DNA methyltransferases, was subjected to RT-PCR analysis. hOAT3 mRNA became detectable in Caco-2 cells after treatment with 5azadC in a concentration-dependent manner (Fig. 8A), whereas no induction of hOAT3 mRNA was observed in HepG2 or HEK293 cells (data not shown). In HEK293 cells, however, transient transfection of HNF1α alone or cotransfection of HNF1α and HNF1β followed by treatment with 100 μM 5azadC elicited de novo expression of hOAT3 mRNA, whereas transfection of HNF1β alone was not sufficient to induce hOAT3 expression (Fig. 8B). These data suggest that the repression mechanism of the hOAT3 gene in hOAT3-nonexpressing cells involves DNA methylation and that synergism between HNF1α or HNF1β expression and DNA demethylation may be required for the transcription of this gene.

Discussion

In the present study, the transcriptional regulation of the hOAT3 gene was characterized for the first time. The promoter region required for basal promoter activity was deter-

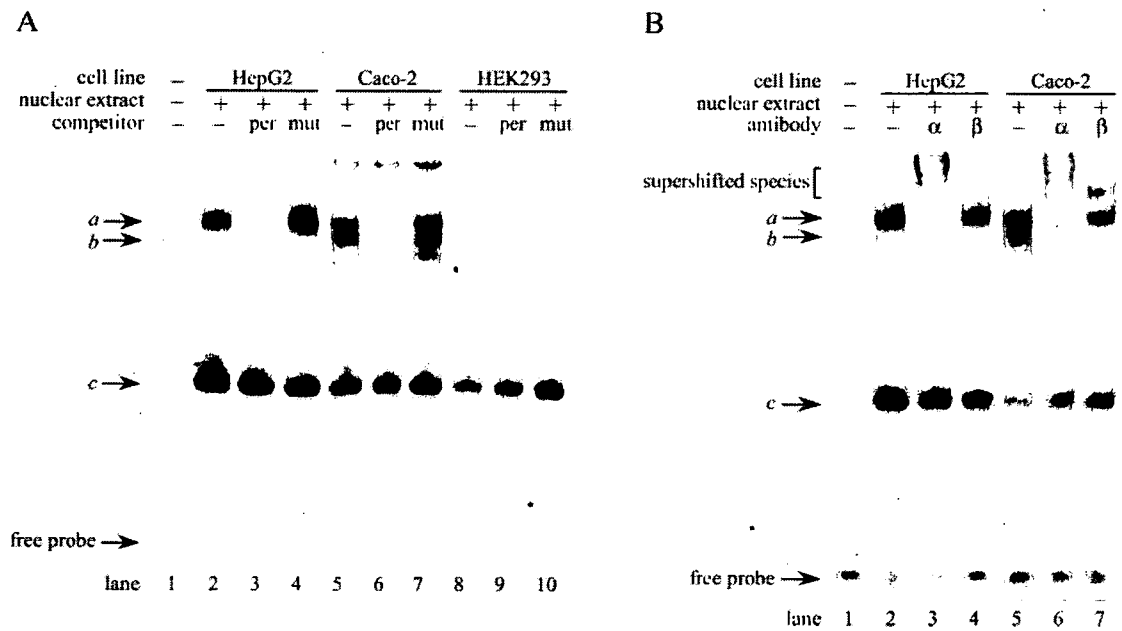

Fig. 6. Electrophoretic mobility shift assay using the oligonucleotide probe corresponding to the −76/−41 region and nuclear extracts from HepG2, Caco-2, and HEK293 cells. A, competition assays. Digoxigenin-labeled probe (Table 1) was incubated with nuclear extracts from HepG2, Caco-2, and HEK293 cells in the presence or absence of a 25-fold excess of unlabeled competitor (per or mut) as indicated. B, supershift analysis. The probe was incubated with nuclear extracts from HepG2 and Caco-2 cells in the presence or absence of a specific antibody against HNF1α (α) or HNF1β (β) as indicated. The DNA-protein complex was detected as described under *Materials and Methods*.

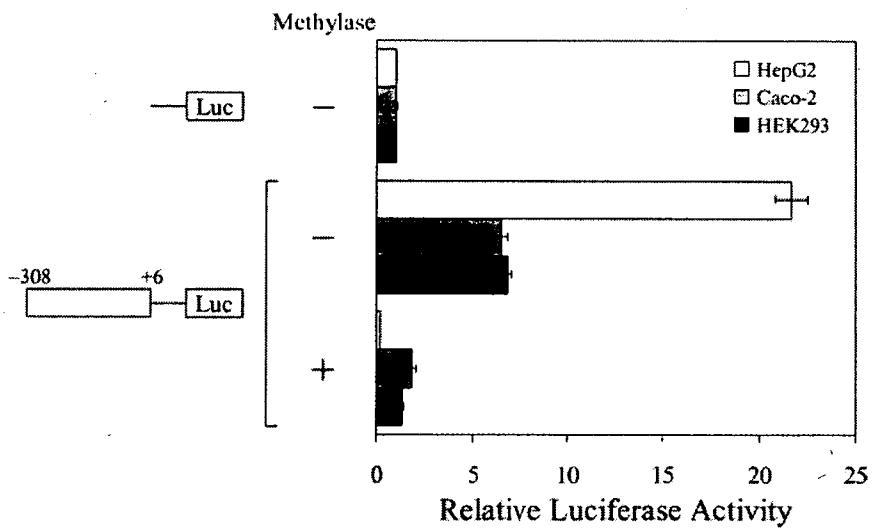

Fig. 7. Effect of in vitro methylation on the hOAT3 promoter activity. hOAT3 −308/+6 promoter construct was methylated in vitro with SssI methylase and transfected into HepG2 (white bars), Caco-2 (gray bars), and HEK293 cells (black bars). The luciferase activity was measured as described under *Materials and Methods* and was shown as the factor of induction over background activity measured in cells transfected with pGL3-Basic without methylation in each cell line. Results are presented as the mean ± S.E. of triplicate samples.

mined using a series of deleted promoter-reporter constructs (Fig. 2), and the region extending from −308 to +6 relative to the transcriptional start site was found to be important for promoter activity. An almost 70% homologous sequence over 300 base pairs to the hOAT3 minimal promoter was found in the mouse and rat Oat3 genomic locus. A database search with Mat Inspector revealed that the TATA motif and HNF1 motif are conserved among species as depicted in Fig. 1, suggesting the importance of these elements in the regulation of OAT3 genes.

The contribution of HNF1α and HNF1β to the basal promoter activity of the hOAT3 gene was demonstrated by several in vitro studies. Mutations in the hOAT3 minimal promoter HNF1 motif resulted in an approximately 50% reduction in the luciferase activity compared with the wild-type construct in HepG2 and Caco-2 cells, but not in HEK293 cells (Fig. 4), which is consistent with the different expression pattern of HNF1α and HNF1β in these cell lines (Fig. 3). The residual activity of the mutated construct may be ascribed to the transactivation by other factors, the binding of which is also affected by DNA methylation, because in vitro methylation of the minimal promoter construct almost abolished its activity (Fig. 7). The amount or contribution of these unknown factors in HEK293 cells may be higher than that in Caco-2 cells, because the luciferase activity of the hOAT3 minimal promoter in HEK293 cells is similar to that in Caco-2 cells regardless of the absence of HNF1α and HNF1β. Further studies will be required to identify these factors that are also required for the transcription of hOAT3. Cotransfection of HNF1α and/or HNF1β dramatically enhanced the hOAT3 wild-type promoter-driven luciferase activity in HEK293 cells, whereas the luciferase activity driven by the mutated promoter was unaffected (Fig. 5). Binding of HNF1α or HNF1β to the HNF1 binding motif in the hOAT3 promoter was confirmed by electrophoretic mobility shift assays (Fig. 6A). Supershift analysis using specific antibodies for HNF1α and HNF1β suggested that the protein complex binding to this region is HNF1α/HNF1α homodimer or HNF1α/HNF1β heterodimer (Fig. 6B). These data indicate that HNF1α, HNF1β, or both are critical for hOAT3 gene expression, although the transactivation potency of HNF1β is lower than that of HNF1α (Fig. 5). It seems that the transcription of mOat3 is also under the control of HNF1α and HNF1β. The involvement of HNF1α and HNF1β in regulation of the OAT3 gene is conserved among species, further supporting a critical role for these transcription factors in the regulation of the hOAT3 and mOat3 genes.

hOAT3 is predominantly expressed in the kidney and only weakly in the brain and skeletal muscle (Cha et al., 2001; Alebouyeh et al., 2003). Moreover, in the kidney, the expression is restricted to the proximal tubules. Consistent with the distribution of hOAT3 in the kidney, HNF1α expression is primarily detected in the proximal tubules, whereas HNF1β is expressed throughout all segments of the nephron, from the proximal tubules to the collecting ducts (Lazzaro et al., 1992; Pontoglio et al., 1996). However, it should be noted that the tissue distribution of HNF1α and HNF1β is much wider than that of hOAT3 (Blumenfeld et al., 1991; Rey-Campos et al., 1991). In addition to the kidney, they are expressed in the liver, intestine, stomach, and pancreas where hOAT3 is not expressed. Therefore, the tissue-specific and region-restricted expression of hOAT3 cannot be accounted for only by HNF1α and/or HNF1β, and other mechanisms must be involved in the regulation of hOAT3 expression.

Because multiple CpG dinucleotides are located in the hOAT3 minimal promoter region (Fig. 1), the involvement of DNA methylation in the regulation of hOAT3 expression was investigated. The transcriptional activity of the hOAT3 minimal promoter was suppressed by in vitro methylation of the reporter construct (Fig. 7). The expression of hOAT3, normally silent in Caco-2 and HEK293 cells, was activated de novo by DNA demethylation in Caco-2 cells, and by the transient transfection of HNF1α or cotransfection of HNF1α and HNF1β together with the DNA demethylation in HEK293 cells (Fig. 8). However, the expression of hOAT3 in HEK293 cells transfected with HNF1β alone followed by DNA demethylation with 5azadC was below the detection limit, although independent transfection of HNF1β enhanced the luciferase activity of hOAT3 wild-type reporter construct (Fig. 5). This could be due to the lower transactivation potency of the HNF1β/HNF1β homodimer. On the other hand, there was no induction of hOAT3 mRNA in HepG2 cells by 5azadC treatment, regardless of the presence of endogenous HNF1α and HNF1β. The lack of inducibility of hOAT3 expression in HepG2 may be accounted for by the presence of negative regulatory factors observed predominantly in HepG2 cells in the luciferase assays (Fig. 2) and/or the absence of other transcription factors necessary for de novo

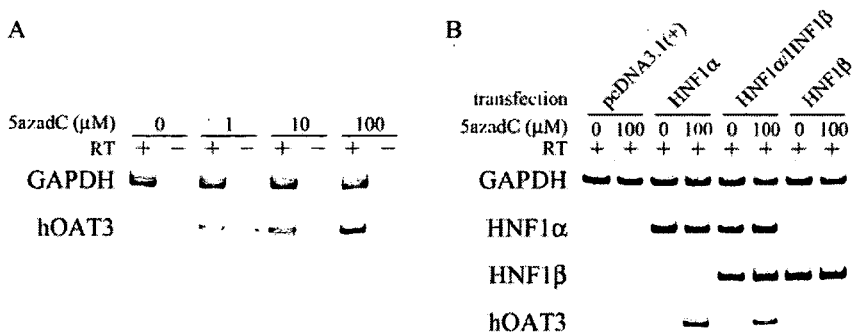

Fig. 8. Reactivation of the hOAT3 expression in hOAT3-negative cells. A, expression profile of hOAT3 mRNA in 5azadC-treated Caco-2 cells. The expression of GAPDH and hOAT3 mRNA was determined by RT-PCR in Caco-2 cells cultured for 72 h with 0, 1, 10, or 100 μM 5azadC. B, expression profile of hOAT3 mRNA in HEK293 cells transfected with HNF1α and/or HNF1β together with 5azadC treatment. The expression of GAPDH, HNF1α, HNF1β, and hOAT3 mRNA was determined by RT-PCR in HEK293 cells transiently transfected with 0.5 μg/well pcDNA3.1(+), 0.5 μg/well HNF1α, 0.25 μg/well HNF1α and HNF1β, or 0.5 μg/well HNF1β, followed by treatment with 0 or 100 μM 5azadC for 48 h. Results with the PCR templates with reverse transcription (RT +) are shown. No amplified products were detected from the templates without reverse transcription (data not shown).

expression of hOAT3. Further analysis will be required for the identification of these factors. Taken together, these observations indicate that the expression of hOAT3 is negatively regulated by DNA methylation.

There have been several reports regarding the involvement of DNA methylation in tissue-specific gene expression (Cho et al., 2001; Imamura et al., 2001; Futscher et al., 2002; Hattori et al., 2004; Jin et al., 2005). It is possible that the minimal promoter region of hOAT3 is hypermethylated in the tissues where the expression of hOAT3 is not detected, such as liver and intestine. The hypermethylation of the promoter region may render the neighboring chromatin structure inaccessible for many transcription factors, including HNF1α and HNF1β, through deacetylation of histones. Thus, regardless of the expression of HNF1α and HNF1β, the expression of hOAT3 is suppressed in those tissues.

The mechanism underlying the proximal tubule-restricted expression of hOAT3 in the kidney is more complicated. The nuclear extracts from the kidney normally contain HNF1α/HNF1β heterodimers and HNF1β/HNF1β homodimers (Pontoglio et al., 1996), and the results of the supershift experiments suggest that the protein complex binding to the HNF1 motif of hOAT3 might be the HNF1α/HNF1α homodimer or HNF1α/HNF1β heterodimer (Fig. 6B). It is likely that the promoter region of hOAT3 is hypomethylated in the kidney proximal tubules, enabling the HNF1α/HNF1β heterodimers to bind to their recognition sites. This model is supported by the results showing that the expression of hOAT3 was induced by cotransfection of HNF1α and HNF1β with the concomitant DNA demethylation in HEK293 cells (Fig. 8B). The methylation status in the other nephron segments is debatable. The promoter region may be hypermethylated in the whole nephron except for the proximal tubules, resulting in the suppression of hOAT3 expression. A second possibility is that although the promoter region is not highly methylated, interaction with the HNF1β/HNF1β homodimer is not sufficient to evoke the hOAT3 expression as observed in Fig. 8B.

Taking all these findings into consideration, it seems that the tissue specificity of the expression of hOAT3 may be explained by the coordinated action of genetic (HNF1α and HNF1β) and epigenetic (DNA methylation) mechanisms. Analysis of the Oat3 expression in HNF1α-null mice (Pontoglio et al., 1996; Lee et al., 1998) will show the relative contribution of HNF1α in vivo. In addition, direct demonstration of the difference in the DNA methylation and chromatin status in the hOAT3 promoter region among in vivo tissues/cells will be required in future studies.

The tissue distribution of mOat3 and rOat3 is not consistent with that of hOAT3: they are expressed not only in the kidney but also in the liver and the brain (Kusuhara et al., 1999; Kikuchi et al., 2003; Ohtsuki et al., 2004). It is noteworthy that the positions of the CpG dinucleotides in the hOAT3 promoter are not conserved in the corresponding region of mouse and rat Oat3 (Fig. 1). The difference in the contribution of epigenetic factors to the regulation of OAT3 gene expression may explain the species difference in the expression patterns, because the contribution of genetic factors seems to be comparable as far as HNF1α and HNF1β are concerned.

Despite the numerous studies of the genes regulated by HNF1α or HNF1β, there are few reports regarding the mechanism whereby these homeodomain proteins can bind to the promoter region of their target genes or transactivate the expression in a tissue-specific manner. Here, we have provided the first evidence suggesting that the methylation profile of the promoter or the chromatin configuration of the target genes determines the accessibility of HNF1α and HNF1β. The synergistic action of the chromatin structure in the promoter region and binding of HNF1α and HNF1β could be a critical clue to the further understanding of the tissue-specific gene regulation by these two transcription factors. Future studies are needed to investigate whether this scheme is applicable to other genes.

In conclusion, the present study provides a clear demonstration that the expression of hOAT3 is positively regulated by HNF1α and HNF1β and negatively regulated by DNA methylation. This is the first demonstration of the importance of HNF1α and HNF1β in the regulation of genes indispensable for detoxification in the kidney. Furthermore, it is also suggested that the coordinated action of genetic and epigenetic factors might explain the tissue-specific expression of hOAT3.

References

Alebouyeh M, Takeda M, Onozato ML, Tojo A, Noshiro R, Hasannejad H, Inatomi J, Narikawa S, Huang XL, Khamdang S, et al. (2003) Expression of human organic anion transporters in the choroid plexus and their interactions with neurotransmitter metabolites. *J Pharmacol Sci* **93**:430–436.

Bai Y, Pontoglio M, Hiesberger T, Sinclair AM, and Igarashi P (2002) Regulation of kidney-specific Ksp-cadherin gene promoter by hepatocyte nuclear factor-1beta. *Am J Physiol* **283**:F839–F851.

Barbacci E, Reber M, Ott MO, Breillat C, Huetz F, and Cereghini S (1999) Variant hepatocyte nuclear factor 1 is required for visceral endoderm specification. *Development* **126**:4795–4805.

Bird A (2002) DNA methylation patterns and epigenetic memory. *Genes Dev* **16**:6–21.

Blumenfeld M, Maury M, Chouard T, Yaniv M, and Condamine H (1991) Hepatic nuclear factor 1 (HNF1) shows a wider distribution than products of its known target genes in developing mouse. *Development* **113**:589–599.

Cha SH, Sekine T, Fukushima JI, Kanai Y, Kobayashi Y, Goya T, and Endou H (2001) Identification and characterization of human organic anion transporter 3 expressing predominantly in the kidney. *Mol Pharmacol* **59**:1277–1286.

Cheret C, Doyen A, Yaniv M, and Pontoglio M (2002) Hepatocyte nuclear factor 1 alpha controls renal expression of the Npt1-Npt4 anionic transporter locus. *J Mol Biol* **322**:929–941.

Cho JH, Kimura H, Minami T, Ohgane J, Hattori N, Tanaka S, and Shiota K (2001) DNA methylation regulates placental lactogen I gene expression. *Endocrinology* **142**:3389–3396.

Coffinier C, Gresh L, Fiette L, Tronche F, Schutz G, Babinet C, Pontoglio M, Yaniv M, and Barra J (2002) Bile system morphogenesis defects and liver dysfunction upon targeted deletion of HNF1beta. *Development* **129**:1829–1838.

Coffinier C, Thepot D, Babinet C, Yaniv M, and Barra J (1999) Essential role for the homeoprotein vHNF1/HNF1beta in visceral endoderm differentiation. *Development* **126**:4785–4794.

Eraly SA, Vallon V, Vaughn DA, Gangoiti JA, Richter K, Nagle M, Monte JC, Rieg T, Truong DM, Long JM, et al. (2006) Decreased renal organic anion secretion and plasma accumulation of endogenous organic anions in OAT1 knock-out mice. *J Biol Chem* **281**:5072–5083.

Futscher BW, Oshiro MM, Wozniak RJ, Holtan N, Hanigan CL, Duan H, and Domann FE (2002) Role for DNA methylation in the control of cell type specific maspin expression. *Nat Genet* **31**:175–179.

Gresh L, Fischer E, Reimann A, Tanguy M, Garbay S, Shao X, Hiesberger T, Fiette L, Igarashi P, Yaniv M, et al. (2004) A transcriptional network in polycystic kidney disease. *EMBO (Eur Mol Biol Organ) J* **23**:1657–1668.

Hasegawa M, Kusuhara H, Endou H, and Sugiyama Y (2003) Contribution of organic anion transporters to the renal uptake of anionic compounds and nucleoside derivatives in rat. *J Pharmacol Exp Ther* **305**:1087–1097.

Hasegawa M, Kusuhara H, Sugiyama D, Ito K, Ueda S, Endou H, and Sugiyama Y (2002) Functional involvement of rat organic anion transporter 3 (rOat3; Slc22a8) in the renal uptake of organic anions. *J Pharmacol Exp Ther* **300**:746–753.

Hattori N, Nishino K, Ko YG, Ohgane J, Tanaka S, and Shiota K (2004) Epigenetic control of mouse Oct-4 gene expression in embryonic stem cells and trophoblast stem cells. *J Biol Chem* **279**:17063–17069.

Imamura T, Ohgane J, Ito S, Ogawa T, Hattori N, Tanaka S, and Shiota K (2001) CpG island of rat sphingosine kinase-1 gene: tissue-dependent DNA methylation status and multiple alternative first exons. *Genomics* **76**:117–125.

Jin B, Seong JK, and Ryu DY (2005) Tissue-specific and de novo promoter methylation of the mouse glucose transporter 2. *Biol Pharm Bull* **28**:2054–2057.

Jung D, Hagenbuch B, Gresh L, Pontoglio M, Meier PJ, and Kullak-Ublick GA (2001) Characterization of the human OATP-C (SLC21A6) gene promoter and regulation of liver-specific OATP genes by hepatocyte nuclear factor 1 α. *J Biol Chem* **276**:37206–37214.

Kikuchi R, Kusuhara H, Sugiyama D, and Sugiyama Y (2003) Contribution of organic anion transporter 3 (Slc22a8) to the elimination of *p*-aminohippuric acid and benzylpenicillin across the blood-brain barrier. *J Pharmacol Exp Ther* **306:** 51–58.

Kusuhara H, Sekine T, Utsunomiya-Tate N, Tsuda M, Kojima R, Cha SH, Sugiyama Y, Kanai Y, and Endou H (1999) Molecular cloning and characterization of a new multispecific organic anion transporter from rat brain. *J Biol Chem* **274:**13675–13680.

Lazzaro D, De Simone V, De Magistris L, Lehtonen E, and Cortese R (1992) LFB1 and LFB3 homeoproteins are sequentially expressed during kidney development. *Development* **114:**469–479.

Lee YH, Sauer B, and Gonzalez FJ (1998) Laron dwarfism and non-insulin-dependent diabetes mellitus in the Hnf-1alpha knockout mouse. *Mol Cell Biol* **18:**3059–3068.

Lowry OH, Rosebrough NJ, Farr AL, and Randall RJ (1951) Protein measurement with the folin phenol reagent. *J Biol Chem* **193:**265–275.

Mendel DB and Crabtree GR (1991) HNF-1, a member of a novel class of dimerizing homeodomain proteins. *J Biol Chem* **266:**677–680.

Mendel DB, Hansen LP, Graves MK, Conley PB, and Crabtree GR (1991) HNF-1 alpha and HNF-1 beta (vHNF-1) share dimerization and homeo domains, but not activation domains, and form heterodimers in vitro. *Genes Dev* **5:**1042–1056.

Ohtsuki S, Kikkawa T, Mori S, Hori S, Takanaga H, Otagiri M, and Terasaki T (2004) Mouse reduced in osteosclerosis transporter functions as an organic anion transporter 3 and is localized at abluminal membrane of blood-brain barrier. *J Pharmacol Exp Ther* **309:**1273–1281.

Pontoglio M, Barra J, Hadchouel M, Doyen A, Kress C, Bach JP, Babinet C, and Yaniv M (1996) Hepatocyte nuclear factor 1 inactivation results in hepatic dysfunction, phenylketonuria, and renal Fanconi syndrome. *Cell* **84:**575–585.

Pontoglio M, Prie D, Cheret C, Doyen A, Leroy C, Froguel P, Velho G, Yaniv M, and Friedlander G (2000) HNF1alpha controls renal glucose reabsorption in mouse and man. *EMBO (Eur Mol Biol Organ) Rep* **1:**359–365.

Rey-Campos J, Chouard T, Yaniv M, and Cereghini S (1991) vHNF1 is a homeoprotein that activates transcription and forms heterodimers with HNF1. *EMBO (Eur Mol Biol Organ) J* **10:**1445–1457.

Robertson EE and Rankin GO (2005) Human renal organic anion transporters: characteristics and contributions to drug and drug metabolite excretion. *Pharmacol Ther* **109:**399–412.

Sekine T, Miyazaki H, and Endou H. 2006. Molecular physiology of renal organic anion transporters. *Am J Physiol* **290:**F251–F261.

Shih DQ, Bussen M, Sehayek E, Ananthanarayanan M, Shneider BL, Suchy FJ, Shefer S, Bollileni JS, Gonzalez FJ, Breslow JL, et al. (2001) Hepatocyte nuclear factor-1alpha is an essential regulator of bile acid and plasma cholesterol metabolism. *Nat Genet* **27:**375–382.

Shiota K (2004) DNA methylation profiles of CpG islands for cellular differentiation and development in mammals. *Cytogenet Genome Res* **105:**325–334.

Sweet DH, Miller DS, Pritchard JB, Fujiwara Y, Beier DR, and Nigam SK (2002) Impaired organic anion transport in kidney and choroid plexus of organic anion transporter 3 (*Oat3* (*Slc22a8*)) knockout mice. *J Biol Chem* **277:**26934–26943.

Tronche F and Yaniv M (1992) HNF1, a homeoprotein member of the hepatic transcription regulatory network. *Bioessays* **14:**579–587.

Van Aubel RA, Masereeuw R, and Russel FG (2000) Molecular pharmacology of renal organic anion transporters. *Am J Physiol* **279:**F216–F232.

Address correspondence to: Dr. Yuichi Sugiyama, Department of Molecular Pharmacokinetics, Graduate School of Pharmaceutical Sciences, The University of Tokyo, 7-3-1 Hongo, Bunkyo-ku, Tokyo 113-0033, Japan. E-mail: sugiyama@mol.f.u-tokyo.ac.jp

0090-9556/07/3502-209–214$20.00
DRUG METABOLISM AND DISPOSITION
Copyright © 2007 by The American Society for Pharmacology and Experimental Therapeutics
DMD 35:209–214, 2007

Vol. 35, No. 2
12567/3169331
Printed in U.S.A.

Involvement of Breast Cancer Resistance Protein (BCRP/*ABCG2*) in the Biliary Excretion and Intestinal Efflux of Troglitazone Sulfate, the Major Metabolite of Troglitazone with a Cholestatic Effect

Junichi Enokizono, Hiroyuki Kusuhara, and Yuichi Sugiyama

Graduate School of Pharmaceutical Sciences, University of Tokyo, Tokyo, Japan

Received August 27, 2006; accepted November 1, 2006

ABSTRACT:

Troglitazone sulfate (TGZS) is the major metabolite of troglitazone (TGZ), an antidiabetic agent, and thought to be a cause of the cholestasis induced by TGZ. The aim of the present study is to elucidate the involvement of breast cancer resistance protein (BCRP/*ABCG2*) in the hepatic disposition of TGZS. The basal-to-apical transport of TGZS was enhanced in organic anion transporting polypeptide 1B1-expressing Madin-Darby canine kidney II cells by infection of recombinant adenovirus harboring human BCRP and mouse Bcrp cDNA. TGZS was given to wild-type and Bcrp (−/−) mice by constant infusion. Biliary excretion is the predominant elimination pathway of TGZS in wild-type mice, and the biliary excretion clearance of TGZS with regard to the hepatic concentration was reduced to 30% of the control in Bcrp (−/−) mice. However, plasma and hepatic concentrations were unchanged, suggesting induction of compensatory mechanisms in Bcrp (−/−) mice for the elimination of TGZS. Involvement of BCRP in the intestinal efflux transport of TGZS was examined using everted sacs. The mucosal efflux clearance of TGZS showed only a slight reduction (15% reduction) in Bcrp (−/−) mice. Our results suggest that BCRP plays a major role in the biliary excretion but a minor role in the intestinal transport of TGZS.

Troglitazone (TGZ) (Fig. 1a) was the first marketed thiazolidinedione, and it has been used for the treatment of type 2 hyperglycemia. It can sensitize tissues to insulin by activating peroxisome proliferator-activated receptor-γ, thereby inhibiting glucose release from hepatocytes and enhancing the insulin-dependent glucose metabolism in adipose tissue and skeletal muscle (reviewed in Chen, 1998). However, TGZ was withdrawn from the market in 2000 because of idiosyncratic severe hepatotoxicity. A great deal of research was carried out on the hepatotoxicity of TGZ, and multiple mechanisms were proposed, such as the production of reactive intermediates and direct mitochondrial injury (reviewed in Smith, 2003). An alternative mechanism that has been proposed is cholestasis. Cholestasis was observed in patients with severe hepatotoxicity (Fukano et al., 2000; Menon et al., 2001), and Funk et al. (2001b) showed that a single bolus administration of TGZ increased the plasma bile acid concentration in rats. Because troglitazone sulfate (TGZS) (Fig. 1b), the major metabolite of TGZ, is a more potent inhibitor of the bile salt export pump (BSEP) than TGZ, and the hepatic concentration of TGZS was much greater than that of TGZ (Funk et al., 2001b), TGZS has been hypothesized to account for the cholestatic effect of TGZ. A gender difference in the cholestatic effect of TGZ in rats was related to the sex-dependent formation of TGZS: the formation of TGZS was greater in male rats, which exhibit more severe cholestasis (Funk et al., 2001a). Based on these findings, it has been speculated that TGZS increases the likelihood of hepatotoxicity induced by TGZ. In addition to the conjugation rate, the hepatic elimination mechanism of TGZS will be important for hepatotoxicity. Elucidation of the molecular mechanism of the hepatic disposition of TGZS is also important to obtain a clue to account for the idiosyncratic hepatotoxicity of TGZ. Polymorphisms or mutations of the enzymes and transporters may be associated with this idiosyncrasy.

TGZS is produced mainly by sulfotransferase (SULT) 1A1 in the liver and is predominantly excreted into the bile (Kawai et al., 1997; Honma et al., 2002). Almost 50% was recovered in the bile as unchanged form after intraduodenum administration of TGZS in rats (Kawai et al., 2000). As far as hepatic uptake is concerned, Nozawa et al. (2004) showed that TGZS is transported by organic anion transporting polypeptide (OATP) 1B1 and OATP1B3, and OATP1B1 transported TGZS more efficiently than OATP1B3 (Nozawa et al., 2004). OATP1B1 will play a major role in the hepatic uptake of TGZS. As far as the biliary excretion process is concerned, Kostrubsky et al. (2001) investigated the involvement of multidrug resistance-

This study was supported by Health and Labour Sciences Research Grants for Research on Regulatory Science of Pharmaceuticals and Medical Devices from Ministry of Health, Labour, and Welfare for the Research on Advanced Medical Technology.

Article, publication date, and citation information can be found at http://dmd.aspetjournals.org.

doi:10.1124/dmd.106.012567.

ABBREVIATIONS: TGZ, troglitazone; TGZS, troglitazone sulfate; BSEP, bile salt excrete pump; SULT, sulfotransferase; OATP, organic anion transporting polypeptide; MRP2/Mrp2, multidrug resistance-associated protein 2; BCRP/Bcrp, breast cancer resistance protein; ME3277, sodium hydrogen {4-[(4,5,6,7-tetrahydrothieno {3,2-c} pyridin-2-yl) carbonylamino] acetyl-o-phenylene} dioxydiacetate; MDCKII, Madin-Darby canine kidney II; GFP, green fluorescent protein; mBcrp, mouse Bcrp; hBCRP, human BCRP; PBS, phosphate-buffered saline; LC/MS, liquid chromatography/mass spectrometry; BSA-KRB, bovine serum albumin/Krebs-Ringer bicarbonate; SNP, single nucleotide polymorphism(s).

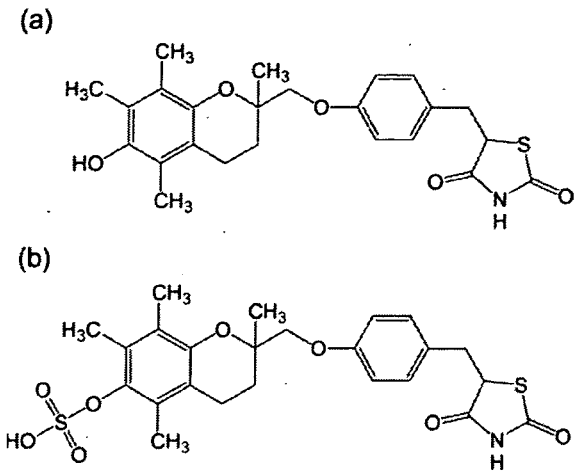

FIG. 1. Chemical structures of TGZ (A) and TGZS (B).

associated protein 2 (MRP2/*ABCC2*) in the biliary excretion of TGZS using TR$^-$ rats, a mutant strain with an inherited deficiency in MRP2. The biliary excretion of TGZS was delayed in TR$^-$ rats compared with normal rats; however, the amount of TGZS excreted into the bile was not markedly reduced in TR$^-$ rats (Kostrubsky et al., 2001). One explanation of this is that other transporters are also involved in the biliary excretion of TGZS. The transport system involved in the intestinal reabsorption of TGZS remains to be identified.

Breast cancer resistance protein (BCRP/*ABCG2*) is a member of the ATP-binding cassette transporter family. BCRP is ubiquitously expressed in normal tissues, and cumulative studies using Bcrp (−/−) mice have shown the importance of BCRP in the urinary excretion, secretion into milk and tissue, and fetal distribution of xenobiotics (Maliepaard et al., 2001; Jonker et al., 2002, 2005). In the liver and intestine, BCRP is localized in the canalicular and brush-border membranes, respectively, and it mediates the biliary excretion of nitrofurantoin and pitavastatin and limits the oral absorption of topotecan, 2-amino-1-methyl-6-phenylimidazo[4,5-b]pyridine, and ME3277 (Jonker et al., 2002; van Herwaarden et al., 2003; Hirano et al., 2005; Kondo et al., 2005; Merino et al., 2005). The substrate specificity of BCRP is characterized by the acceptance of a variety of sulfate conjugates (Suzuki et al., 2003), and BCRP plays a significant role in the efflux transport of certain kinds of sulfate conjugates in the small intestine and kidney (Mizuno et al., 2004; Adachi et al., 2005). Therefore, we hypothesized that BCRP plays a critical role in the prevention of TGZ-induced cholestasis by facilitating biliary excretion, and investigated the contribution of BCRP to the biliary and intestinal excretion of TGZS using Bcrp (−/−) mice.

Materials and Methods

Materials and Animals. TGZ and TGZS were gifts from Sankyo Co. Ltd. (Tokyo, Japan). All the other chemicals were commercially available and of reagent grade. A 24-well Transwell (6.5-mm diameter, 0.4-μm pore size) was purchased from Corning Costar (Bodenheim, Germany). Male Bcrp (−/−) mice (Jonker et al., 2002) and wild-type FVB mice used in the present study were 9 to 16 weeks old and weighed 25 to 33 g. The animals were maintained under controlled temperature with a light/dark cycle of 12 h. Food and water were available ad libitum.

Transcellular Transport Study. The transcellular transport study was performed as previously reported with minor modifications (Matsushima et al., 2005). In brief, Madin-Darby canine kidney II (MDCKII) cells expressing human OATP1B1 (MDCKII/OATP1B1) were grown on the Transwell membrane for 3 days in Dulbecco's modified Eagle's medium (Invitrogen, Carlsbad, CA) with 10% fetal bovine serum (Sigma-Aldrich, St. Louis, MO) and 1% antibiotic-antimycotic solution (Sigma-Aldrich). The cells were infected with the recombinant adenovirus harboring green fluorescent protein (GFP), mouse Bcrp (mBcrp), or human BCRP (hBCRP) expression vector at an infection multiplicity of 200. The details of the construction of these recombinant adenoviruses were described in a previous report (Kondo et al., 2004). After 2 days of culture, the cells were used for transport studies. The cells were preincubated in Krebs-Henseleit buffer (142 mM NaCl, 23.8 mM Na_2CO_3, 4.83 mM KCl, 0.96 mM KH_2PO_4, 1.20 mM $MgSO_4$, 12.5 mM HEPES, 5 mM glucose, and 1.53 mM $CaCl_2$, pH 7.4) for 30 min, and then transport experiments were initiated by replacing the medium on one side of the cell monolayer with Krebs-Henseleit buffer containing 3 μM TGZS. At appropriate times (1, 2, and 3 h), 100-μl aliquots were taken from the opposite side of the cell monolayer and replaced with 100 μl of buffer. After the last sampling, the cell monolayers were solubilized with 500 μl of 0.2 M NaOH and then neutralized with 100 μl of 1 M HCl. The protein concentration was measured by the Lowry method.

The flux of TGZS across cell monolayers was calculated as follows: Flux (μl/mg protein) = $(C_{acceptor} \times V_{acceptor})/(C_{donor} \times$ protein amount), where $C_{acceptor}$ is the TGZS concentration in the acceptor solution, $V_{acceptor}$ is the volume of the acceptor solution, and C_{donor} is the initial TGZS concentration in the donor solution (3 μM). The flux was plotted against time, and the efflux clearances (μl/h/mg protein) were calculated from the slopes.

Determination of Biliary Excretion of TGZS in Wild-Type and Bcrp (−/−) Mice. Under urethane anesthesia (1.25 g/kg, i.p.), the right jugular vein was cannulated with a polyethylene tube (PE-10; Becton Dickinson, Franklin Lakes, NJ) for injection of TGZS. After abdominal dissection, the gallbladder was ligated, and the bile duct was cannulated with a polyethylene tube (UT-3; Unique Medical, Tokyo, Japan) to collect bile. TGZS was injected at a dose of 0.5 μmol/kg, followed by continuous infusion at a dose rate of 0.1 μmol/h/kg. Blood samples were collected from the left jugular vein at 60, 80, 100, and 120 min. The blood samples were heparinized and centrifuged to obtain plasma samples. Bile samples were collected at 20-min intervals between 60 and 120 min postdosing. Immediately after the last blood and bile sampling, mice were sacrificed, and the liver was removed. The liver was homogenized with a 9-fold volume of phosphate-buffered saline (PBS) to obtain a 10% liver homogenate.

The plasma samples (5 μl) were mixed with 20 μl of PBS and 75 μl of acetonitrile; the bile samples (1 μl) were mixed with 49 μl of PBS and 100 μl of acetonitrile; and the liver homogenates (10 μl) were mixed with 40 μl of PBS and 100 μl of acetonitrile. All these mixed solutions were centrifuged at 15,000*g* for 10 min. The supernatants (plasma sample, 80 μl; bile and liver sample, 10 μl) were evaporated, and the pellets were reconstituted with 20% acetonitrile (plasma sample, 80 μl; bile and liver sample, 200 μl) and subjected to liquid chromatography/mass spectrometry (LC/MS) analysis.

Determination of Urinary Excretion of TGZS in Wild-Type and Bcrp (−/−) Mice. Under urethane anesthesia (1.25 g/kg, i.p.), the right jugular vein was cannulated with a polyethylene tube (PE-10) for injection of TGZS, and the urinary bladder was cannulated with two polyethylene tubes (PE-50; Becton Dickinson). One cannula was fitted with a syringe filled with saline to wash the inside of the urinary bladder, and the other cannula was used for the collection of urine and wash solution. TGZS was injected at a dose of 0.5 μmol/kg followed by continuous infusion at a dose rate of 0.1 μmol/h/kg. Mannitol was concomitantly infused at a dose rate of 160 mg/h/kg to increase the urine volume. Urine samples were collected at 20-min intervals between 60 and 120 min. After every collection of urine, the bladder was flushed with about 300 μl of saline, and the wash solution was added to the urine. The urine samples (50 μl) were mixed with 150 μl of acetonitrile and centrifuged at 15,000*g* for 10 min. The supernatants (100 μl) were evaporated, and the pellets were reconstituted in 20% acetonitrile (100 μl) and subjected to LC/MS analysis.

Everted Sac Study. Mice were anesthetized with ether and sacrificed by exsanguination from the femoral artery and vein. Immediately after sacrifice, the ileum was dissected. The ileum was ligated at one end and then everted. The open end of the everted ileum was ligated after the insertion of a polyethylene tube (SP-45; Natsume, Tokyo, Japan) to make a 5-cm-long sac. Krebs-Ringer buffer (350 μl) containing 0.3% bovine serum albumin (BSA-KRB, pH 6.4) was added to the serosal side of the everted sac via the cannula, and the everted sacs were incubated at 37°C in 10 ml of BSA-KRB. After a 10-min preincubation, the everted sacs were placed in BSA-KRB containing

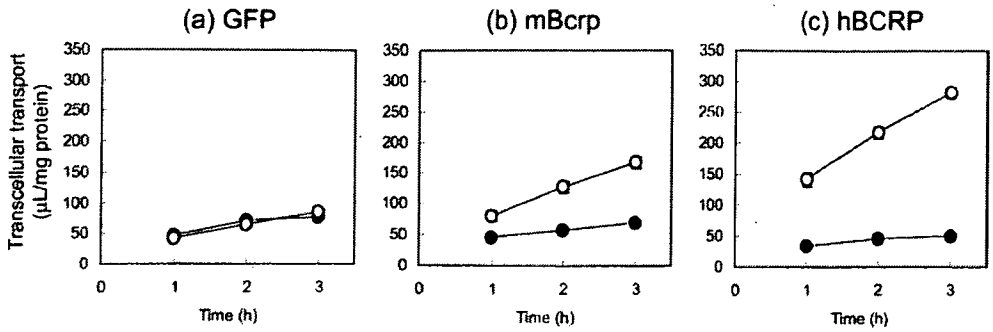

FIG. 2. The transcellular transport of TGZS across monolayers of MDCKII/OATP1B1 expressing GFP, mBcrp, and hBCRP. The transport in the apical-to-basal direction is represented by closed circles and that in the basal-to-apical direction by open circles. Data are represented by mean values ± S.E. of triplicate experiments.

10 μM TGZ and incubated again at 37°C. Aliquots (200 μl) were collected from the mucosal side at 15, 30, 45, and 60 min after incubation with TGZ. After the last sampling, the serosal solution was removed, and the everted sacs were rinsed with ice-cold PBS. Throughout the entire procedure, the mucosal solution was bubbled with O_2/CO_2 (95:5) gas.

The aliquots (75 μl) from the mucosal solution were mixed with acetonitrile (75 μl) and centrifuged at 15,000*g* for 10 min. The supernatants were subjected to LC/MS analysis. The tissue samples were weighed and homogenized with a 9-fold volume of PBS to give 10% tissue homogenates. The tissue homogenates (50 μl) were mixed with acetonitrile (75 μl) and centrifuged at 15,000*g* for 10 min, and the supernatants were subjected to LC/MS analysis.

LC/MS Analysis. An LC/MS-2010 EV equipped with a Prominence LC system (Shimadzu, Kyoto, Japan) was used for the analysis. Samples were separated on a CAPCELL PAK C18 MGII column (3 μm, 2 × 50 mm; Shiseido, Tokyo, Japan) in binary gradient mode. For the mobile phase, 10 mM acetic ammonium and acetonitrile were used. The acetonitrile concentration was initially 23%, then linearly increased up to 70% over 1.5 min, and kept at 70% for a further 1 min. Finally, the column was re-equilibrated at an acetonitrile concentration of 23% for 2.5 min. The total run time was 5 min. TGZS was eluted at 3 min using this method. In the mass analysis, TGZS was detected at a mass-to-charge ratio of 520 under negative electron spray ionization conditions. The interface voltage was −3.5 kV, and the nebulizer gas (N_2) flow was 1.5 l/min. The heat block and curved desolvation line temperatures were 200 and 150°C, respectively.

Data Analysis of Biliary Excretion. Because the plasma and biliary excretion was almost constant between 60 and 120 min (Fig. 3), the plasma and liver concentrations at 120 min were assumed to be steady-state concentrations. Total clearance (CL_{tot}) was calculated by dividing the infusion rate by the plasma concentration at 120 min. The biliary excretion clearance based on the plasma concentration ($CL_{bile, plasma}$) was calculated by dividing the biliary excretion rate in the last time segment (100–120 min) by the plasma concentration at 120 min. The biliary excretion clearance based on the liver concentration ($CL_{bile, liver}$) was calculated by dividing the biliary excretion rate in the last time segment by the liver concentration at 120 min. The fraction of the biliary excretion was calculated by dividing the biliary excretion rate in the last time segment by the infusion rate.

Efflux Transport in Everted Sac Study. The mucosally excreted amounts of TGZS per unit length of tissue were calculated as follows: Mucosal excretion = ($C_{mucosal} \times V_{mucosal}$)/tissue length, where $C_{mucosal}$ is the TGZS concentration in the mucosal solution, $V_{mucosal}$ is the volume of the mucosal solution (10 ml), and the tissue length was 5 cm. The excreted amounts of TGZS in the mucosal side were plotted against the incubation time (Fig. 4a), and the mucosal efflux rates were estimated from the slope. Mucosal efflux clearances ($CL_{mucosal}$) were calculated by dividing the mucosal efflux rates by the tissue concentrations assuming that 1 g of intestine = 1 ml.

Statistical Analysis. Statistical analysis for significant differences was performed using the two-tailed Student's *t* test or one-way analysis of variance, followed by the Tukey multiple comparison test. A probability of <0.05 was considered to be statistically significant.

Results

In Vitro Transport Study of TGZS in BCRP-Expressed Cells. BCRP-mediated transport of TGZS was examined using GFP-, mBcrp-, and hBCRP-expressed MDCKII/OATP1B1 cells. Figure 2 shows the time courses of the transcellular transport of TGZS in GFP-, mBcrp-, and hBCRP-expressed cell systems. The transport of TGZS increased linearly up to 3 h, suggesting that the initial rates were maintained up to the end of the experiments. The transport rates are summarized in Table 1. The apical-to-basal transport was significantly reduced in hBCRP-expressed cells compared with that in GFP cells. The basal-to-apical transport was significantly increased in both mBcrp- and hBCRP-expressed cells. The ratios of basal-to-apical/apical-to-basal flux were 3.6 and 9.3 in MDCK II cells expressing OATP1B1/mBcrp and OATP1B1/hBCRP, respectively, whereas that in GFP-expressed cells was almost symmetric (flux ratio was 1.45).

TABLE 1

Kinetic parameters of the transcellular transport of TGZS across the monolayers of MDCKII/OATP1B1 cells expressing GFP, mBcrp, and hBCRP

The data are represented by mean values ± S.E. of triplicate experiments. Statistical significance was analyzed by one-way analysis of variance followed by Tukey multiple comparison test.

	Efflux Clearance		Flux Ratio (Basal-to-Apical/ Apical-to-Basal)
	Apical-to-Basal	Basal-to-Apical	
	μl/h/mg protein		
GFP	15.1 ± 0.2	21.9 ± 0.8	1.45 ± 0.06
mBcrp	12.2 ± 3.9	43.9 ± 1.2***	3.60 ± 1.15
hBCRP	7.57 ± 1.01**	70.5 ± 2.8***,†††	9.31 ± 1.30

** $P < 0.01$ and *** $P < 0.001$ statistical differences in efflux clearances with those in GFP-expressed cells.

††† $P < 0.001$ statistical difference in efflux clearances between mBcrp- and hBCRP-expressed cells.

Effect of BCRP on the Biliary Excretion of TGZS. The biliary excretion study was performed by continuous infusion with a priming dose to achieve steady-state conditions. The biliary excretion, plasma, and liver concentrations of TGZS are shown in Fig. 3. The bile flow was almost the same in wild-type and Bcrp (−/−) mice (38.5 ± 4.6 versus 41.8 ± 5.4 μl/min/kg). The plasma concentrations and the biliary excretion of TGZS became almost constant between 60 and 120 min. The plasma concentrations showed a slight reduction in Bcrp (−/−) mice; however, the differences were not statically significant. The biliary excretion of TGZS was markedly reduced in Bcrp (−/−) mice at all the time periods. There was no significant difference in the liver concentrations between wild-type and Bcrp (−/−) mice. The pharmacokinetic parameters are shown in Table 2. The total clearance was slightly increased in Bcrp (−/−) mice, but this was not statistically significant. The biliary excretion clearances based on the plasma and liver concentrations were markedly reduced in Bcrp (−/−) mice to about 30% of those in wild-type mice. The biliary excretion of TGZS was almost 100% in wild-type mice, whereas that in Bcrp (−/−) mice was 32.6%. These results indicate that there is another elimination process for TGZS in Bcrp (−/−) mice. To investigate this, the urinary excretion of TGZS was examined in Bcrp (−/−) mice. However, TGZS concentrations in all the urine samples were

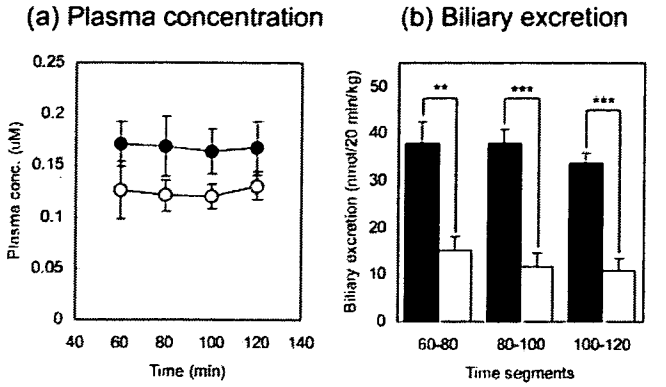

FIG. 3. The effect of BCRP on the biliary excretion of TGZS. a, the time courses of the plasma concentrations of TGZS. b, the biliary excretion of TGZS. c, the liver concentrations of TGZS at 120 min postdosing. The data in wild-type mice are shown by closed circles or columns and those in Bcrp (−/−) mice by open circles or columns. All the data are represented by mean values ± S.E. of four mice. Asterisks represent statistically significant differences between wild-type and Bcrp (−/−) mice; **, $P < 0.01$ and ***, $P < 0.001$.

TABLE 2

Pharmacokinetic parameters of TGZS in the in vivo biliary excretion study

The data are represented by mean values ± S.E. of four mice.

Animal	CL_{total}	$CL_{bile, plasma}$	$CL_{bile, liver}$	Fraction of Biliary Excretion
	ml/min/kg			%
Wild-type	10.6 ± 1.4	10.9 ± 1.9	0.148 ± 0.017	102 ± 6
Bcrp (−/−)	13.3 ± 1.4	4.15 ± 0.86*	0.0424 ± 0.0115**	32.6 ± 7.9***

* $P < 0.05$, ** $P < 0.01$, and *** $P < 0.001$ statistical significance between wild-type and Bcrp (−/−) mice analyzed by two-tailed Student's *t* test.

below the lower limit of quantification (10 nM). Because the volume of the urine sample (urine + wash solution) was less than 450 μl at every 20-min period, the urinary excretion rate of TGZS was considered to be less than 0.45 nmol/h/kg. This means that the urinary excretion of TGZS is less than 1% of the dose in Bcrp (−/−) mice.

Effect of BCRP on the Mucosal Efflux Transport of TGZS in Everted Sacs. The effect of BCRP on the mucosal efflux transport of TGZS was examined by using everted ileum sacs. TGZ was added to the mucosal side, and the mucosal efflux of the intracellularly formed TGZS was determined. The results are shown in Fig. 4. The time courses of the mucosal efflux of TGZS were linear, suggesting that the initial rates were maintained up to the end of the experiments. The mucosal efflux was slightly reduced in Bcrp (−/−) mice (Fig. 4a). The tissue concentrations of TGZS at the end of the experiments were similar between wild-type and Bcrp (−/−) mice (Fig. 4b). The mucosal efflux clearance showed a significant but only slight reduction (15.3% decrease) in Bcrp (−/−) mice (Fig. 4c).

Discussion

The present study is focused on the involvement of BCRP in the biliary and intestinal excretion of TGZS. We first examined whether TGZS is a substrate of BCRP in vitro using a BCRP-expressed MDCKII/OATP1B1 system where OATP1B1 and BCRP are localized in the basal and apical membrane, respectively, and the basal-to-apical transport of their common substrates is increased (Matsushima et al., 2005). Compared with GFP-expressed cells, the basal-to-apical transport was increased in mBcrp- and hBCRP-expressed cells, suggesting that TGZS is a substrate of both mBcrp and hBCRP. A higher flux ratio was observed in hBCRP-expressed cells than in mBcrp-expressed cells, suggesting that hBCRP transports TGZS more efficiently than mBcrp.

In the in vivo study, there was no significant difference in bile flow between in wild-type and Bcrp (−/−) mice. The bile flow obtained in the present study was about 40 μl/min/kg and within the range of previously reported bile flows in FVB male mice (28.7 and 61 μl/min/kg) (Wang et al., 2001; Werner et al., 2002). These results suggested that cholestasis was not induced under the present experimental conditions. Funk et al. (2001b) showed the cholestatic effect of TGZ in rats. In that report, the plasma and liver concentrations of TGZS were 110 and 260 μM, respectively, much higher than those in the present study (plasma, 0.1–0.2 μM; liver, 10–15 μM). This suggests that the plasma and liver concentrations of TGZS in the present study were too low to induce cholestasis.

Comparison of the total body and biliary excretion clearances showed that biliary excretion is the main elimination pathway of TGZS in wild-type mice. The biliary excretion of TGZS was markedly reduced in Bcrp (−/−) mice, and $CL_{bile, liver}$, which represents the intrinsic efflux ability at the canalicular membrane, was reduced in Bcrp (−/−) mice to 29% of that in wild-type mice. Therefore, BCRP is the major transporter involved in the biliary excretion of TGZS. Cumulative studies using Mrp2-deficient mutant rats have shown that MRP2 accounts for the biliary excretion of some sulfate conjugates, such as tauro-conjugated bile acid sulfate, phenolphthalein sulfate, and acetaminophen sulfate (Takikawa et al., 1991; Akimoto et al., 2001; Tanaka et al., 2003; Zamek-Gliszczynski et al., 2005). Very recently, Zamek-Gliszczynski et al. (2006) showed that BCRP is also involved in the biliary excretion of sulfate conjugates, including 4-methylumbelliferone sulfate, acetaminophen sulfate, and harmol sulfate, using Bcrp (−/−) mice. These results suggest that BCRP and MRP2 are two major transporters responsible for the biliary excretion of sulfate conjugates, and BCRP makes a major contribution to the biliary excretion of xenobiotic sulfate conjugates. In humans, the biliary excretion of TGZS may be mediated by BCRP because hBCRP transports TGZS more efficiently than mBcrp.

The total clearance and hepatic concentration were not changed in Bcrp (−/−) mice, although biliary excretion is the predominant elimination pathway in wild-type mice. At steady state, the biliary excretion accounts for, at most, 30% of the total body clearance in Bcrp (−/−) mice, and the remaining fraction could be explained by other elimination mechanisms that were induced to compensate for the loss of biliary excretion. Urinary excretion could be an alternative elimination pathway of TGZS. However, the urinary excretion of TGZS was negligible in Bcrp (−/−) mice. Therefore, induction of hepatic metabolic enzymes is a likely mechanism. Currently, there is no information regarding the enzymes that are induced in Bcrp (−/−) mice, and further studies are necessary to identify them.

The effect of BCRP on the intestinal reabsorption was examined using everted ileum sacs. The mucosal efflux clearance ($CL_{mucosal}$) of TGZS represents the intrinsic efflux ability of TGZS in the brush-border membrane of the intestinal epithelial cells, and the effect of BCRP on the mucosal excretion of TGZS can be measured by a comparison of $CL_{mucosal}$ between wild-type and Bcrp (−/−) mice. The $CL_{mucosal}$ of TGZS showed only a slight reduction in Bcrp (−/−)

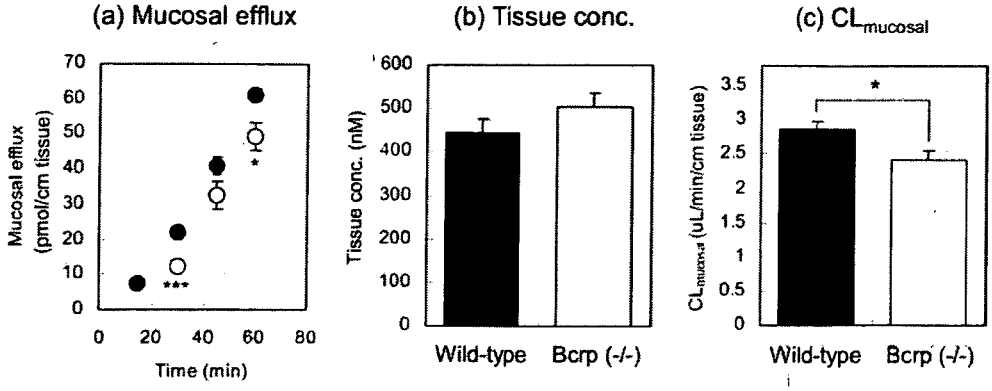

FIG. 4. The effect of BCRP on the intestinal transport of TGZS in everted ileum sacs. a, the time courses of the mucosal efflux of TGZS. b, the tissue concentrations of TGZS after a 60-min incubation. c, the mucosal efflux clearances of TGZS. The data in wild-type mice are shown by closed circles or columns and those in Bcrp (−/−) mice by open circles or columns. All the data are represented by mean values ± S.E. of four everted sacs independently prepared from four mice. Asterisks represent statically significant differences between wild-type and Bcrp (−/−) mice; *, $P < 0.05$ and ***, $P < 0.001$.

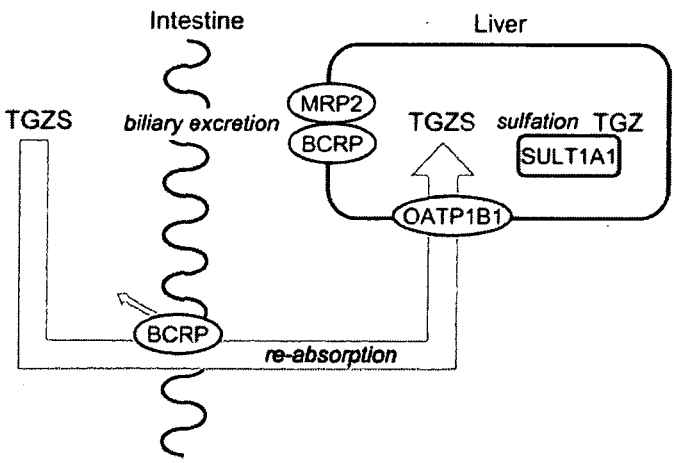

FIG. 5. Schematic representation of the molecular mechanism involved in the hepatic disposition of TGZS.

mice. This result suggests that BCRP plays only a limited role in preventing oral absorption of TGZS.

Figure 5 summarizes the molecular mechanism involved in the hepatic disposition of TGZS. TGZS is produced by SULT1A1 from TGZ and is excreted into the bile mainly by BCRP. TGZS excreted into the intestinal lumen undergoes reabsorption into the circulating blood (Kawai et al., 2000). SULT1A1, BCRP, and OATP1B1 are the important molecules controlling the hepatic disposition of TGZS. BCRP has some functional single nucleotide polymorphisms (SNP), such as C376T (Q126stop), C421A (Q141K), and G1322A (S441N). The C376T mutation introduces a stop codon, resulting in the production of truncated BCRP (Imai et al., 2002). The C421A allele is associated with a reduction in the protein level (Imai et al., 2002; Kondo et al., 2004; Kobayashi et al., 2005). The G1322A allele affects both the protein level and localization of BCRP (Kondo et al., 2004). Among these SNP, C421A exhibits the highest frequency (about 10 and 30% in Caucasian and Japanese, respectively) (Kobayashi et al., 2005). Clinical studies revealed that the plasma exposure of diflomotecan, topotecan, and rosuvastatin was higher in subjects carrying the C421A allele (Sparreboom et al., 2004, 2005; Zhang et al., 2006). These functional SNP of BCRP may increase the liver and/or plasma exposure of TGZS, affecting the susceptibility to TGZS if any induction of compensatory mechanisms, which were observed in Bcrp (−/−) mice but do not occur in humans. Besides BCRP, SULT1A1 and OATP1B1 also have functional SNP (Raftogianis et al., 1997; Nowell et al., 2002; Nishizato et al., 2003; Mwinyi et al., 2004; Wegman et al., 2005; Maeda et al., 2006). A combination of these functional SNP in BCRP, SULT1A1, and OATP1B1 may be involved in the idiosyncratic hepatotoxicity of TGZ.

In conclusion, our present study revealed that TGZS is a substrate of mBcrp and hBCRP and that the biliary excretion of TGZS is mainly mediated by BCRP in mice.

Acknowledgments. We thank Sankyo Co. Ltd. for supplying us with TGZ and TGZS, Dr. Kazuya Maeda and Soichiro Matsushima for providing MDCK cells expressing OATP1B1, and Dr. Alfred H. Schinkel (The Netherlands Cancer Institute, The Netherlands) for supplying Bcrp (−/−) mice.

References

Adachi Y, Suzuki H, Schinkel AH, and Sugiyama Y (2005) Role of breast cancer resistance protein (Bcrp1/Abcg2) in the extrusion of glucuronide and sulfate conjugates from enterocytes to intestinal lumen. *Mol Pharmacol* **67**:923–928.

Akimoto K, Sano N, and Takikawa H (2001) Biliary excretion of tauroursodeoxycholate-3-sulfate in the rat. *Steroids* **66**:701–705.

Chen C (1998) Troglitazone: an antidiabetic agent. *Am J Health Syst Pharm* **55**:905–925.

Fukano M, Amano S, Sato J, Yamamoto K, Adachi H, Okabe H, Fujiyama Y, and Bamba T (2000) Subacute hepatic failure associated with a new antidiabetic agent, troglitazone: a case report with autopsy examination. *Hum Pathol* **31**:250–253.

Funk C, Pantze M, Jehle L, Ponelle C, Scheuermann G, Lazendic M, and Gasser R (2001a) Troglitazone-induced intrahepatic cholestasis by an interference with the hepatobiliary export of bile acids in male and female rats. Correlation with the gender difference in troglitazone sulfate formation and the inhibition of the canalicular bile salt export pump (Bsep) by troglitazone and troglitazone sulfate. *Toxicology* **167**:83–98.

Funk C, Ponelle C, Scheuermann G, and Pantze M (2001b) Cholestatic potential of troglitazone as a possible factor contributing to troglitazone-induced hepatotoxicity: in vivo and in vitro interaction at the canalicular bile salt export pump (Bsep) in the rat. *Mol Pharmacol* **59**:627–635.

Hirano M, Maeda K, Matsushima S, Nozaki Y, Kusuhara H, and Sugiyama Y (2005) Involvement of BCRP (ABCG2) in the biliary excretion of pitavastatin. *Mol Pharmacol* **68**:800–807.

Honma W, Shimada M, Sasano H, Ozawa S, Miyata M, Nagata K, Ikeda T, and Yamazoe Y (2002) Phenol sulfotransferase, ST1A3, as the main enzyme catalyzing sulfation of troglitazone in human liver. *Drug Metab Dispos* **30**:944–949.

Imai Y, Nakane M, Kage K, Tsukahara S, Ishikawa E, Tsuruo T, Miki Y, and Sugimoto Y (2002) C421A polymorphism in the human breast cancer resistance protein gene is associated with low expression of Q141K protein and low-level drug resistance. *Mol Cancer Ther* **1**:611–616.

Jonker JW, Buitelaar M, Wagenaar E, Van Der Valk MA, Scheffer GL, Scheper RJ, Plosch T, Kuipers F, Elferink RP, Rosing H, et al. (2002) The breast cancer resistance protein protects against a major chlorophyll-derived dietary phototoxin and protoporphyria. *Proc Natl Acad Sci USA* **99**:15649–15654.

Jonker JW, Merino G, Musters S, van Herwaarden AE, Bolscher E, Wagenaar E, Mesman E, Dale TC, and Schinkel AH (2005) The breast cancer resistance protein BCRP (ABCG2) concentrates drugs and carcinogenic xenotoxins into milk. *Nat Med* **11**:127–129.

Kawai K, Hirota T, Muramatsu S, Tsuruta F, Ikeda T, Kobashi K, and Nakamura KI (2000) Intestinal absorption and excretion of troglitazone sulphate, a major biliary metabolite of troglitazone. *Xenobiotica* **30**:707–715.

Kawai K, Kawasaki-Tokui Y, Odaka T, Tsuruta F, Kazui M, Iwabuchi H, Nakamura T, Kinoshita T, Ikeda T, Yoshioka T, et al. (1997) Disposition and metabolism of the new oral antidiabetic drug troglitazone in rats, mice and dogs. *Arzneimittelforschung* **47**:356–368.

Kobayashi D, Ieiri I, Hirota T, Takane H, Maegawa S, Kigawa J, Suzuki H, Nanba E, Oshimura M, Terakawa N, et al. (2005) Functional assessment of ABCG2 (BCRP) gene polymorphisms to protein expression in human placenta. *Drug Metab Dispos* **33**:94–101.

Kondo C, Onuki R, Kusuhara H, Suzuki H, Suzuki M, Okudaira N, Kojima M, Ishiwata K, Jonker JW, and Sugiyama Y (2005) Lack of improvement of oral absorption of ME3277 by prodrug formation is ascribed to the intestinal efflux mediated by breast cancer resistant protein (BCRP/ABCG2). *Pharm Res (NY)* **22**:613–618.

Kondo C, Suzuki H, Itoda M, Ozawa S, Sawada J, Kobayashi D, Ieiri I, Mine K, Ohtsubo K, and Sugiyama Y (2004) Functional analysis of SNPs variants of BCRP/ABCG2. *Pharm Res (NY)* **21**:1895–1903.

Kostrubsky VE, Vore M, Kindt E, Burliegh J, Rogers K, Peter G, Altrogge D, and Sinz MW

(2001) The effect of troglitazone biliary excretion on metabolite distribution and cholestasis in transporter-deficient rats. *Drug Metab Dispos* **29**:1561–1566.

Maeda K, Ieiri I, Yasuda K, Fujino A, Fujiwara H, Otsubo K, Hirano M, Watanabe T, Kitamura Y, Kusuhara H, et al. (2006) Effects of organic anion transporting polypeptide 1B1 haplotype on pharmacokinetics of pravastatin, valsartan, and temocapril. *Clin Pharmacol Ther* **79**:427–439.

Maliepaard M, Scheffer GL, Faneyte IF, van Gastelen MA, Pijnenborg AC, Schinkel AH, van De Vijver MJ, Scheper RJ, and Schellens JH (2001) Subcellular localization and distribution of the breast cancer resistance protein transporter in normal human tissues. *Cancer Res* **61**:3458–3464.

Matsushima S, Maeda K, Kondo C, Hirano M, Sasaki M, Suzuki H, and Sugiyama Y (2005) Identification of the Hepatic efflux transporters of organic anions using double-transfected madin-darby canine kidney II cells expressing human organic anion-transporting polypeptide 1B1 (OATP1B1)/multidrug resistance-associated protein 2, OATP1B1/multidrug resistance 1, and OATP1B1/breast cancer resistance protein. *J Pharmacol Exp Ther* **314**:1059–1067.

Menon KVN, Angulo P, and Lindor KD (2001) Severe cholestatic hepatitis from troglitazone in a patient with nonalcoholic steatohepatitis and diabetes mellitus. *Am J Gastroenterol* **96**:1631–1634.

Merino G, Jonker JW, Wagenaar E, van Herwaarden AE, and Schinkel AH (2005) The breast cancer resistance protein (BCRP/ABCG2) affects pharmacokinetics, hepatobiliary excretion, and milk secretion of the antibiotic nitrofurantoin. *Mol Pharmacol* **67**:1758–1764.

Mizuno N, Suzuki M, Kusuhara H, Suzuki H, Takeuchi K, Niwa T, Jonker JW, and Sugiyama Y (2004) Impaired renal excretion of 6-hydroxy-5,7-dimethyl-2-methylamino-4-(3-pyridylmethyl) benzothiazole (E3040) sulfate in breast cancer resistance protein (BCRP1/ABCG2) knockout mice. *Drug Metab Dispos* **32**:898–901.

Mwinyi J, Johne A, Bauer S, Roots I, and Gerloff T (2004) Evidence for inverse effects of OATP-C (SLC21A6) 5 and 1b haplotypes on pravastatin kinetics. *Clin Pharmacol Ther* **75**:415–421.

Nishizato Y, Ieiri I, Suzuki H, Kimura M, Kawabata K, Hirota T, Takane H, Irie S, Kusuhara H, Urasuki Y, et al. (2003) Polymorphisms of OATP-C (SLC21A6) and OAT3 (SLC22A8) genes: consequences for pravastatin pharmacokinetics. *Clin Pharmacol Ther* **73**:554–565.

Nowell S, Sweeney C, Winters M, Stone A, Lang NP, Hutchins LF, Kadlubar FF, and Ambrosone CB (2002) Association between sulfotransferase 1A1 genotype and survival of breast cancer patients receiving tamoxifen therapy. *J Natl Cancer Inst* **94**:1635–1640.

Nozawa T, Sugiura S, Nakajima M, Goto A, Yokoi T, Nezu J, Tsuji A, and Tamai I (2004) Involvement of organic anion transporting polypeptides in the transport of troglitazone sulfate: implications for understanding troglitazone hepatotoxicity. *Drug Metab Dispos* **32**:291–294.

Ott P, Ranek L, and Young MA (1998) Pharmacokinetics of troglitazone, a PPAR-gamma agonist, in patients with hepatic insufficiency. *Eur J Clin Pharmacol* **54**:567–571.

Raftogianis RB, Wood TC, Otterness DM, Van Loon JA, and Weinshilboum RM (1997) Phenol sulfotransferase pharmacogenetics in humans: association of common SULT1A1 alleles with TS PST phenotype. *Biochem Biophys Res Commun* **239**:298–304.

Smith MT (2003) Mechanisms of troglitazone hepatotoxicity. *Chem Res Toxicol* **16**:679–687.

Sparreboom A, Gelderblom H, Marsh S, Ahluwalia R, Obach R, Principe P, Twelves C, Verweij J, and McLeod HL (2004) Diflomotecan pharmacokinetics in relation to ABCG2 421C>A genotype. *Clin Pharmacol Ther* **76**:38–44.

Sparreboom A, Loos WJ, Burger H, Sissung TM, Verweij J, Figg WD, Nooter K, and Gelderblom H (2005) Effect of ABCG2 genotype on the oral bioavailability of topotecan. *Cancer Biol Ther* **4**:650–658.

Suzuki M, Suzuki H, Sugimoto Y, and Sugiyama Y (2003) ABCG2 transports sulfated conjugates of steroids and xenobiotics. *J Biol Chem* **278**:22644–22649.

Takikawa H, Sano N, Narita T, Uchida Y, Yamanaka M, Horie T, Mikami T, and Tagaya O (1991) Biliary excretion of bile acid conjugates in a hyperbilirubinemic mutant Sprague-Dawley rat. *Hepatology* **14**:352–360.

Tanaka H, Sano N, and Takikawa H (2003) Biliary excretion of phenolphthalein sulfate in rats. *Pharmacology* **68**:177–182.

van Herwaarden AE, Jonker JW, Wagenaar E, Brinkhuis RF, Schellens JH, Beijnen JH, and Schinkel AH (2003) The breast cancer resistance protein (Bcrp1/Abcg2) restricts exposure to the dietary carcinogen 2-amino-1-methyl-6-phenylimidazo[4,5-b]pyridine. *Cancer Res* **63**:6447–6452.

Wang DQ, Paigen B, and Carey MC (2001) Genetic factors at the enterocyte level account for variations in intestinal cholesterol absorption efficiency among inbred stains of mice. *J Lipid Res* **42**:1820–1830.

Wegman P, Vainikka L, Stal O, Nordenskjold B, Skoog L, Rutqvist LE, and Wingren S (2005) Genotype of metabolic enzymes and the benefit of tamoxifen in postmenopausal breast cancer patients. *Breast Cancer Res* **7**:R284–R290.

Werner A, Minich DM, Havinga R, Bloks V, Van Goor H, Kulipers F, and Verkade HJ (2002) Fat malabsorption in essential fatty acid-deficient mice is not due to impaired bile formation. *Am J Physiol* **283**:G900–G908.

Zamek-Gliszczynski MJ, Hoffmaster KA, Tian X, Zhao R, Polli JW, Humphreys JE, Webster LO, Bridges AS, Kalvass JC, and Brouwer KL (2005) Multiple mechanisms are involved in the biliary excretion of acetaminophen sulfate in the rat: role of Mrp2 and Bcrp1. *Drug Metab Dispos* **33**:1158–1165.

Zamek-Gliszczynski MJ, Nezasa K, Tian X, Kalvass JC, Patel NJ, Raub TJ, and Brouwer KL (2006) The important role of Bcrp (Abcg2) in the biliary excretion of sulfate and glucuronide metabolites of acetaminophen, 4-methylumbelliferone, and harmol in mice. *Mol Pharmacol* **70**:2127–2133.

Zhang W, Yu BN, He YJ, Fan L, Li Q, Liu ZQ, Wang A, Liu YL, Tan ZR, Fen J, et al. (2006) Role of BCRP 421C>A polymorphism on rosuvastatin pharmacokinetics in healthy Chinese males. *Clin Chim Acta* **373**:99–103.

Address correspondence to: Yuichi Sugiyama, Graduate School of Pharmaceutical Sciences, The University of Tokyo, 7-3-1, Hongo, Bunkyo-ku, Tokyo 113-0033, Japan. E-mail: sugiyama@mol.f.u-tokyo.ac.jp

EUROPEAN JOURNAL OF PHARMACEUTICAL SCIENCES 27 (2006) 425–446

available at www.sciencedirect.com

SCIENCE DIRECT®

journal homepage: www.elsevier.com/locate/ejps

PHARMACEUTICAL SCIENCES

Review

Transporters as a determinant of drug clearance and tissue distribution

Yoshihisa Shitara[a], *Toshiharu Horie*[a], *Yuichi Sugiyama*[b,*]

[a] *Department of Biopharmaceutics, Graduate School of Pharmaceutical Sciences, Chiba University, 1-8-1, Inohana, Chou-ku, Chiba 260-8675, Japan*

[b] *Department of Molecular Pharmacokinetics, Graduate School of Pharmaceutical Sciences, The University of Tokyo, 7-3-1, Hongo, Bunkyo-ku, Tokyo 113-0033, Japan*

ARTICLE INFO

Article history:
Received 26 October 2005
Received in revised form 1 December 2005
Accepted 6 December 2005

Keywords:
Transporter
Drug elimination
Pharmacokinetics

ABSTRACT

Transporters play an important role in the processes of drug absorption, distribution and excretion. In this review, we have focused on the involvement of transporters in drug excretion in the liver and kidney. The rate of transporter-mediated uptake and efflux determines the rate of renal and hepatobiliary elimination. Transporters are thus important as a determinant of the clearance in the body. Even when drugs ultimately undergo metabolism, their elimination rate is sometimes determined by the uptake rate mediated by transporters. Transporters regulate the pharmacological and/or toxicological effect of drugs because they limit their distribution to tissues responsible for their effect and/or toxicity. For example, the liver-specific distribution of some statins via organic anion transporters helps them to produce their high pharmacological effect. On the other hand, as in the case of metformin taken up by organic cation transporter 1, drug distribution to the tissue(s) may enhance its toxicity. As transporter-mediated uptake is a determinant of the drug elimination rate, drug–drug interactions involving the process of transporter-mediated uptake can occur. In this review, we have introduced some examples and described their mechanisms.

More recently, some methods to analyze such transporter-mediated transport have been reported. The estimation of the contributions of transporters to the net clearance of a drug makes it possible to predict the net clearance from data involving drug transport in transporter-expressing cells. Double transfected cells, where both uptake and efflux transporters are expressed on the same polarized cells, are also helpful for the analysis of the rate of transporter-mediated transcellular transport.

Contents

1. Introduction 426
2. Hepatic and renal transporters as a determinant of drug disposition 428
   2.1. Substrates of hepatobiliary transporters 428
   2.2. Involvement of hepatic uptake transporters in the drug disposition 429

* *Corresponding author.* Tel.: +81 3 5841 4770; fax: +81 3 5800 6949.
E-mail address: sugiyama@mol.f.u-tokyo.ac.jp (Y. Sugiyama).

0928-0987/$ – see front matter © 2005 Elsevier B.V. All rights reserved.
doi:10.1016/j.ejps.2005.12.003

2.2.1. Transporters can be a rate-limiting factor in the elimination of drugs 429
2.2.2. Transporters determine the tissue distribution of drugs 430
2.3. Substrates of renal transporters 432
2.4. The balance of hepatic and renal clearances determine the elimination pathway 432
3. The mechanism of transporter-mediated drug–drug interactions 435
4. A method for estimating the contribution of each transporter to the total hepatic uptake 437
4.1. The importance of the contribution of transporters 437
4.2. Estimation of the contributions of specific transporters to the total hepatic uptake 437
5. Transport studies using double transfected cells 440
6. Conclusion 441
References 441

1. Introduction

Drug elimination in the liver consists of the following processes: (1) hepatic uptake, (2) metabolism and/or (3) biliary excretion (Pang and Rowland, 1977; Pang and Gillette, 1978; Yamazaki et al., 1996a; Shitara et al., 2005). In addition, (4) sinusoidal efflux from the inside of the cell to the blood also determine the hepatic elimination rate. Among these processes, drug transporters are involved in uptake, sinusoidal efflux and biliary excretion (Meier et al., 1997; Kullak-Ublick et al., 2000; van Montfoort et al., 2003; Giacomini and Sugiyama, 2005). Recently, molecular cloning of drug transporters has greatly helped the characterization of the mechanism of drug elimination in the liver (Hagenbuch and Meier, 2003; Keppler and Konig, 2000; Mizuno et al., 2003). It should be noted that hepatic uptake and biliary excretion determine the drug concentration in the liver, and they may affect the pharmacological effects and/or toxic side effects (Giacomini and Sugiyama, 2005). Thus, drug transporters are also a determinant of pharmacological effects and/or side effects for drugs whose target is the liver.

In the kidney, drug clearances are determined by: (1) glomerular filtration, (2) tubular secretion and (3) reabsorption (Inui et al., 2000a,b; Dresser et al., 2001). As glomerular filtration is simply the ultrafiltration of drugs not bound to plasma proteins, no transporters are involved. Transporters are mainly involved in tubular secretion and reabsorption (Koepsell and Endou, 2004; Sekine et al., 2000; Wright and Dantzler, 2004). Several active transport mechanisms have been reported in the proximal tubules and these are involved in secretion. Reabsorption is sometimes mediated by transporters although many drugs are reabsorbed only by passive

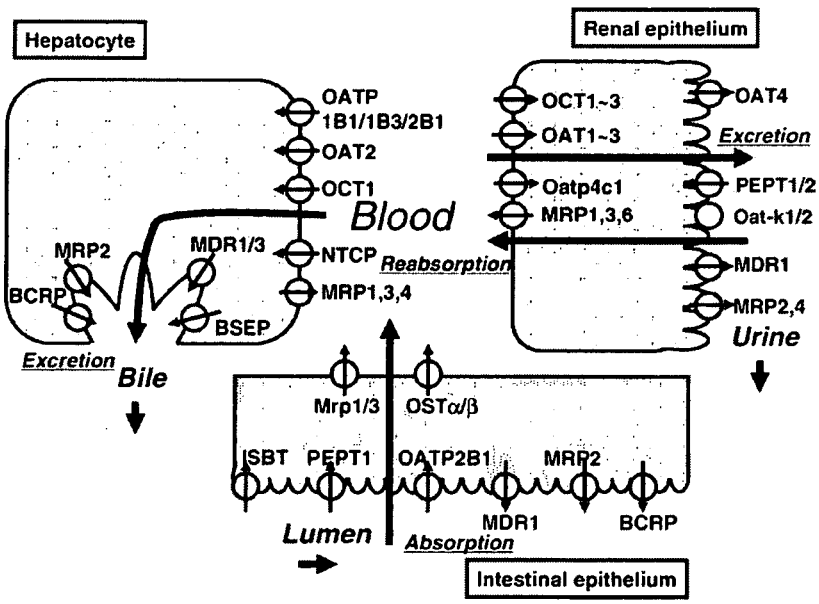

Fig. 1 – Transporters involved in the intestinal absorption, hepatic excretion and renal excretion of drugs. Multiple transporters are involved in the transcellular transport of drugs in the liver, kidney and intestine. For transcellular transport, drugs need to cross two different membranes on the basal and apical sides. In the intestine, drugs are absorbed from the luminal side (brush border membrane) and excreted into the portal blood across the basolateral membrane. In the liver, drugs are taken up into hepatocytes across the sinusoidal membrane and excreted into the bile. In the kidney, drugs undergo secretion (urinary excretion) or reabsorption. In the case of secretion, drugs are taken up from the basolateral side and excreted in the urine across the apical side. However, in the case of reabsorption, drugs are taken up from the urine and excreted in the circulating blood.

diffusion depending on a high drug concentration gradient across the blood and nephron, which is caused by reabsorption of water back into the plasma.

Orally administered drugs firstly pass through the intestine and subsequently appear in the portal blood. This intestinal absorption affects the drug concentration in the circulating blood. Moreover, the intestine functions as a barrier to xenobiotics (Wacher et al., 2001; Zhang and Benet, 2001). In these processes, transporters in intestine play important roles (Ganapathy and Leibach, 1982; Amidon and Lee,

Table 1 – Therapeutic drugs which are substrates of hepatic transporters

		Uptake transporters	Metabolizing enzymes	Bile canalicular tranporters	References
Atorvastatin	Human	OATP1B1	CYP3A4		Kameyama et al. (2005) Lau et al. (2006)
Bosentan	Human		CYP2C9 CYP3A4		
	Rat	Oatp1a1 Oatp1a4 Oatp1b2			Treiber et al. (2004)
Caspofungin	Human	OATP1B1	-		Sandhu et al. (2005)
Cerivastatin	Human	OATP1B1	CYP3A4 CYP2C8		Shitara et al. (2003)
	Rat	Oatp1a1 Oatp1a4 Oatp1b2			Shitara et al. (2004b)
Fexofenadine	Human	OATP1B1[a] OATP1B3 OATP2B1[b]	-	MDR1	Cvetkovic et al. (1999) Niemi et al. (2005a) Shimizu et al. (2005)
	Rat	Oatp1a1 Oatp1a4	-		Cvetkovic et al. (1999)
Glycyrrhizin[c]	Human	OATP1B1 OATP1B3			Ismair et al. (2003)
	Rat	Oatp1a1 Oatp1a4 Oatp1b2			Ismair et al. (2003)
Pravastatin	Human	OATP1B1 OATP2B1	- -	MRP2 BSEP BSEP BCRP MDR1	 Hsiang et al. (1999) Nakai et al. (2001) Sasaki et al. (2002) Kobayashi et al. (2003) Nozawa et al. (2004) Hirono et al. (2005) Matsushima et al. (2005)
	Rat	Oatp1a1 Oatp1a4 Oatp1b2	-	Mrp2	Hsiang et al. (1999) Tokui et al. (1999) Sasaki et al. (2004)
Pitavastatin	Human	OATP1B1 OATP1B3[b]	CYP2C9[b]	MRP2 BCRP MDR1	Hirano et al. (2004, 2005a, 2005b)
Rifampicin	Human	OATP1B1 OATP1B3		MDR1	Schuetz et al. (1996) Vavricka et al. (2002) Tirona et al. (2003)
Repaglinide	Human	OATP1B1	CYP2C8 CYP3A4		Niemi et al. (2005b)
Rosuvastatin	Human	OATP1B1 OATP1B3 OATP2B1	-	MRP2 MDR1 BCRP	Schneck et al. (2004) Kitamura et al. (2005) Huang et al., in press
Telmisartan	Human	OATP1B3	UGTs	MRP2 (as a glucuronide)	Nishino et al. (2000) Ishiguro et al. (2005)

[a] The pharmacokinetics of fexofenadine was altered in subjects with genetic polymorphism of OATP1B1. But the involvement of OATP1B1 in the hepatic uptake of fexofenadine has not been shown directly.
[b] Minor contribution.
[c] Glycyrrhizin is reported only as an inhibitor of uptake transporters.